Chitin-Binding Protein of Verticillium nonalfalfae Disguises Fungus from Plant Chitinases and Suppresses Chitin-Triggered Host Immunity

Volk, Helena; Marton, Kristina; Flajsman, Marko; Radisek, Sebastjan; Tian, Hui; Hein, Ingo

Published in:
Molecular Plant-Microbe Interactions

DOI:
10.1094/MPMI-03-19-0079-R

Publication date:
2019

Document Version
Peer reviewed version

Author Accepted Manuscript of Volk, H, Marton, K, Flajsman, M, Radisek, S, Tian, H, Hein, I, Podlipnik, Č, Thomma, BPHJ, Kosmelj, K, Javornik, B & Berne, S 2019, 'Chitin binding protein of Verticillium nonalfalfae disguises fungus from plant chitinases and supresses chitin-triggered host immunity' Molecular Plant-Microbe Interactions. https://doi.org/10.1094/MPMI-03-19-0079-R ©APS Publications

Chitin binding protein of *Verticillium nonalfalfae* disguises fungus from plant chitinases and supresses chitin-triggered host immunity

Helena Volk[1], Kristina Marton[1], Marko Flajšman[1], Sebastjan Radišek[2], Hui Tian[3], Ingo Hein[4,5], Črtomir Podlipnik[6], Bart P.H.J. Thomma[3], Katarina Košmelj[1], Branka Javornik[1], Sabina Berne[1]

[1]Department of Agronomy, Biotechnical Faculty, University of Ljubljana, Jamnikarjeva 101, SI-1000 Ljubljana, Slovenia; [2]Slovenian Institute of Hop Research and Brewing, Cesta Žalskega tabora 2, SI-3310 Žalec, Slovenia; [3]Laboratory of Phytopathology, Wageningen University and Research, Droevendaalsesteeg 1, 6708 PB Wageningen, the Netherlands, [4]The James Hutton Institute, Invergowrie, Dundee DD2 5DA, Scotland, United Kingdom; [5]The University of Dundee, School of Life Sciences, Division of Plant Sciences at the JHI, Invergowrie, Dundee DD2 5DA, Scotland, United Kingdom; [5]Department of Chemistry and Biochemistry, Faculty of Chemistry and Chemical Technology, University of Ljubljana, Večna pot 113, SI-1000 Ljubljana, Slovenia

Corresponding author: S. Berne; E-mail: sabina.berne@bf.uni-lj.si

Nucleotide sequence data is available under accession numbers MH325205 for *VnaChtBP*, and MH325206 for *VaChtBP*.

Abstract

During fungal infections, plant cells secrete chitinases, which digest chitin in the fungal cell walls. The recognition of released chitin oligomers via lysin motif (LysM)-containing immune host receptors results in the activation of defence signalling pathways. We report here that *Verticillium nonalfalfae*, a hemibiotrophic xylem-invading fungus, prevents these digestion and recognition processes by secreting a CBM18 (carbohydrate binding motif 18)-chitin binding protein, VnaChtBP, which is transcriptionally activated specifically during the parasitic life stages. VnaChtBP is encoded by the *Vna8.213* gene, which is highly conserved within the species, suggesting high evolutionary stability and importance for the fungal lifestyle. In a pathogenicity assay, however, *Vna8.213* knockout mutants exhibit wilting symptoms similar to the wild type fungus, suggesting that *Vna8.213* activity is functionally redundant during fungal infection of hop. In a binding assay, recombinant VnaChtBP binds chitin and chitin oligomers *in vitro* with submicromolar affinity and protects fungal hyphae from degradation by plant chitinases. Moreover, the chitin-triggered production of reactive oxygen species from hop suspension cells was abolished in the presence of VnaChtBP, indicating that VnaChtBP also acts as a suppressor of chitin-triggered immunity.

Using a yeast-two-hybrid assay, circular dichroism, homology modelling and molecular docking, we demonstrated that VnaChtBP forms dimers in the absence of ligands and that this interaction is stabilized by the binding of chitin hexamers with a similar preference in the two binding sites. Our data suggest that, in addition to chitin binding LysM (CBM50) and Avr4 (CBM14) fungal effectors, structurally unrelated CBM18 effectors have convergently evolved to prevent hydrolysis of the fungal cell wall against plant chitinases and to interfere with chitin-triggered host immunity.

Introductory statements

Plant defense against pathogenic organisms relies on innate immunity, which is triggered by recognition of pathogen-derived or endogenous danger signals by plant receptors, described as pattern-triggered immunity (PTI) and effector-triggered immunity (ETI) (Jones and Dangl 2006; Dodds and Rathjen 2010). PTI is activated by host cell surface-localized pattern recognition receptors (PRRs) sensing pathogen- and danger-associated molecular patterns (PAMPs and DAMPs, respectively) (Boller and Felix 2009; Böhm et al. 2014). Pattern recognition receptors, which are either receptor-like kinases (RLKs) or receptor-like proteins (RLPs) that function in conjunction with RLKs, sense PAMPs or DAMPs and transduce downstream signaling to trigger PTI responses. Early PTI responses include the rapid generation of reactive oxygen species, the activation of ion channels and mitogen-activated protein kinases. In turn, this leads to the expression of defense related genes, leading to an accumulation of antimicrobial compounds such as enzymes, which damage pathogen structures, inhibitors of pathogen enzymes and other antimicrobial molecules (Macho and Zipfel 2014; Boller and Felix 2009; Dodds and Rathjen 2010).

PAMPs, released during infection, are conserved molecular patterns characteristic of different pathogen classes (Ranf 2017). In fungi, chitin, in addition to beta-glucan and xylanase, is a well-studied PAMP that activates the host defense response (Sanchez-Vallet et al. 2014). Chitin (a polymer of β-1,4-linked N-acetylglucosamine; $(GlcNAc)_n$), is a major and highly conserved component of fungal cell walls and can be degraded to chitin oligosaccharides by plant apoplastic chitinases (Punja and Zhang 1993; Pusztahelyi 2018). The generated chitin fragments are recognized by a chitin perception system and subsequently activate PTI (Shibuya and Minami 2001; Shinya et al. 2015; Sanchez-Vallet et al. 2014).

Major chitin sensing PRRs, RLKs and RLPs belonging to the LysM domain family, are well studied in *Arabidopsis* and rice (Gust et al. 2012; Ranf 2017). *Arabidopsis* LysM-RLK AtCERK1 (chitin elicitor receptor kinase1) binds N-acetylated chitin fragments with three LysM motifs and, through homodimer formation, mediates chitin-inducible plant defenses (Miya et al. 2007; Liu et al. 2012). Cao et al. (2014) later identified another LysM-RLK in *Arabidopsis*, AtLYK5, which binds chitin at a higher affinity than AtCERK1. The authors propose that AtLYK5 functions as the major chitin receptor, which recruits AtCERK1 to form a chitin inducible receptor complex. In rice, two receptors are involved in chitin triggered immunity (Shimizu et al. 2010). LysM-RLP OsCEBiP (chitin elicitor binding protein) binds N-acetylated chitin fragments, which initiates receptor homodimerization and further heterodimerization with OsCERK1. This heterotetramer formation triggers chitin induced PTI (Hayafune et al. 2014).

To overcome chitin-triggered immunity, successful pathogens have evolved various strategies, including alteration of the composition and structure of cell walls, modification of carbohydrate chains and

secretion of effector proteins to prevent hydrolysis of the fungal cell wall or the release and recognition of chitin oligosaccharides (Sanchez-Vallet et al. 2014).

A well-described strategy of fungal cell wall protection against host chitinases is that of the tomato leaf mold fungus *Cladosporium fulvum,* which secretes chitin-binding protein Avr4 during infection. Avr4 effector binds with its carbohydrate-binding module family 14 (CBM14) to the fungal cell wall chitin and thus shields fungal hyphae against degradation by chitinases (van den Burg et al. 2007; van Esse et al. 2007). There is evidence of a similar protection of cell wall chitin in a phylogenetically closely related species of the Dothideomycete fungi class harboring homologs of Avr4 (Stergiopoulos et al. 2010). Protection of fungal hyphae against hydrolysis by chitinases has also been shown for fungal effectors Mg1LysM and Mg3LysM of *Zymoseptoria tritici* (formerly *M. graminicola*) (Marshall et al. 2011) and Vd2LysM from *Verticillium dahliae* (Kombrink et al. 2017), one of the LysM fungal effectors (de Jonge and Thomma 2009) that are known to bind chitin oligomers via LysM domains or carbohydrate-binding module family 50 (CBM50) (Akcapinar et al. 2015). The first LysM effector, Ecp6, was found in the tomato pathogen *C. fulvum* and its characterization provided evidence that Ecp6 specifically and with high affinity binds chitin oligosaccharides. This competition with receptors subsequently disrupts chitin recognition by host receptors and suppresses the chitin-triggered immune response (Bolton et al. 2008; de Jonge et al. 2010; Sanchez-Vallet et al. 2013). Some fungal genomes contain several genes for LysM effectors and those highly expressed during infection have been characterized in fungal pathogens, including *Z. tritici* (Marshall et al. 2011), *Magnaporthe oryzae* (Mentlak et al. 2012), *Colletotrichum higginsianum* (Takahara et al. 2016) and *V. dahliae* (Kombrink et al. 2017). These studies demonstrate the involvement of LysM effectors in shielding fungal hyphae from chitinases, blocking chitin-induced plant defense responses and in pathogen virulence, or in a combination of these effects.

The question arises of whether there are other molecules/systems/complexes apart from Avr4 (CBM14) and LysM (CBM50) effectors, which can interfere with plant chitin perception and activation of PTI. We have been studying the *Verticillium nonalfalfae* – hop (*Humulus lupulus* L.) pathosystem. In an early comparative transcriptomic study of compatible and incompatible interactions (Cregeen et al. 2015), an *in planta* expressed *V. nonalfalfae* lectin gene was detected. Its relative expression was increasing in susceptible hop cultivar ‘Celeia’ and decreasing in resistant cultivar ‘Wye Target’ over the time course of infection. A preliminary study showed that this *V. nonalfalfae* lectin contains putative carbohydrate-binding module family 18, CBM18 (Wright et al. 1991) domains. CBM18 is a chitin-binding domain involved in recognition of chitin oligomers and typically found in fungal and plant proteins in one or more copies (Lerner and Raikhel 1992). We report here on the characterization of *V. nonalfalfae* lectin with six CBM18 domains and show that it is a novel effector in plant fungal pathogens. VnaChtBP binds chitin, suppresses chitin-triggered production of reactive oxygen species (ROS) in hop and protects hyphae of *Trichoderma viride* from hop chitinases in an *in vitro* protection assay.

Results

The majority of CBM18 module containing proteins of *V. nonalfalfae* are expressed *in planta*

The *Vna8.213* gene, encoding a putative pathogen CBM18-containing chitin binding protein (VnaChtBP), has previously been identified as a differentially expressed transcript during compatible and incompatible interactions of *V. nonalfalfae* and hop (Cregeen et al. 2015). Surveying the *V. nonalfalfae* genome, (Jakše et al. 2018) uncovered ten additional genes that encode for proteins with at least one CBM18 module (Fig. 1). These genes were grouped into four categories according to their domain architecture: Lectin-like proteins (Fig. 1 A), Chitinases (Fig. 1 B), Chitin deacetlyases (Fig. 1 C) and Xyloglucan endotransglucosylase (Fig. 1 D). The size of these proteins ranged between 349 and 1,696 amino acids (Vna6.1 and Vna1.668, respectively) and they harbored between one and ten CBM18 modules. Of these genes, ten are differentially expressed *in planta* (Fig. 1 E) (Marton et al. 2018) and five (Vna2.980, Vna6.6, Vna8.213, Vna9.506 and Vna9.510) were predicted to be classically secreted proteins with N-terminal signal peptides. Of the chitinases (Fig. 1 B), transcripts of *Vna3.655* and *Vna9.506* were detected exclusively in susceptible hop, *Vna1.668* transcripts were found expressed in the roots of both resistant ('Wye Target') and susceptible ('Celeia') hop varieties, while transcripts of *Vna2.980* and *Vna9.510* were barely detectable. Interestingly, only one chitin deacetylase gene (*VnaUn.355*) was expressed during infection, and it showed preferential induction in the roots of both hop varieties. Such an expression profile was also evident for transcripts of *Vna6.6* belonging to xyloglucan endotransglucosylase. The highest expression was observed for *Vna8.213* transcripts, in particular at the late stages of infection of susceptible hop. Interestingly, the *Vna1.667* gene-encoding lectin-like protein, containing 10 CBM18 modules, was barely expressed in the roots of susceptible hop during the early infection stages.

In addition to chitinases (Fig. 1 B), which contain the family 18 glycoside hydrolase domain, one CBM18 and 2-3 CBM50 chitin-binding modules known as LysM domains, another group of protein-like LysM effectors (de Jonge and Thomma 2009) is encoded in the *V. nonalfalfae* genome. Seven genes harboring 1-6 LysM domains were found, four of them with signal peptide and five of them showing expression in infected hops (e-Xtra Fig. S1). The highest expression *in planta* was determined for *Vna2.731*, which is predicted to encode a 19.3 kDa protein with the 1 transmembrane domain and 1 LysM domain and shares 99% identity with the VDBG_03944 protein from *V. alfalfae* VaMs.102.

To confirm the expression patterns of *Vna8.213* measured by RNA-Seq, detailed gene expression profiling of root and shoot samples from susceptible and resistant hop varieties was performed using RT-qPCR at 6, 12 and 18 days post-inoculation (dpi) with *V. nonalfalfae* (Fig. 2). Gene expression of *Vna8.213*, hereinafter designated *VnaChtBP*, increased with time, reaching the highest abundance in stems of susceptible hop at 18 dpi. The overall *VnaChtBP* expression in resistant hop was at a much lower level than in the susceptible variety and peaked at 12 dpi in stems. These results indicate that *VnaChtBP* expression is induced *in planta* and its transcript abundance in susceptible hop increases with the progression of fungal colonization.

Sequence conservation suggests evolutionary stability of *VnaChtBP*

To investigate the presence and sequence variation of *VnaChtBP* in 28 *V. nonalfalfae* isolates (e-Xtra Table S1), PCR amplification and Sanger sequencing of cloned genes was performed. The *VnaChtBP* gene was present in all analyzed isolates and displayed no sequence polymorphisms. This suggests the evolutionary stability of the gene, as well as an important role in the fungal lifestyle.

Among all sequences deposited at NCBI, VnaChtBP shared the highest protein identity with a lectin from *V. alfalfae* (97%; an alfalfa isolate VaMs.102), followed by *V. dahliae* lectin-B (80%; a lettuce isolate VdLs.17), two *V. dahliae* hypothetical proteins, Vd0004_g7043 and Vd0001_g7025 (80% and 79%; strawberry isolates 12161 and 12158), and a hypothetical protein BN1708_012400 from *V. longisporum* (78%; a rapeseed isolate VL1) (e-Xtra Table S2). Additional homologs (e-Xtra File S1), but with lower identity (48-39%), were identified in fungi amongst Sordariomyceta (40) and Dotideomyceta (3), and in fungi *Incertae sedis* amongst Neocallimastigomycetes (5) and Chytridiomycetes (2).

Because of the high sequence similarity shared between VnaChtBP and *V. alfalfae* VaMs.102 lectin, PCR screening and Sanger sequencing of amplicons from four additional *V. alfalfae* isolates was carried out. As with *VnaChtBP*, no allelic polymorphisms were found among the sequences obtained and comparison of *V. nonalfalfae* and *V. alfalfae* gene sequences from these isolates also showed 97% sequence identity. Within the 36 single nucleotide polymorphisms identified, only 13 resulted in amino acid substitutions (e-Xtra File S2).

VnaChtBP binds chitin *in vitro* and protects fungal hyphae against plant chitinases

V. nonalfalfae VnaChtBP is an intronless gene and predicted to encode for a cysteine rich (12.5%) apoplastic effector (VnaChtBP) with 400 amino acids, including N-terminal signal peptide and six type 1 Chitin binding domains (ChtBD1; PF00187). This domain is classified in the CAZY database (Lombard et al. 2014) as Carbohydrate-binding module 18 (CBM18) and consists of 30 to 43 residues rich in glycines and cysteines, which are organized in a conserved four-disulfide core (Andersen et al. 1993; Asensio et al. 2000; Wright et al. 1991). It is a common structural motif, with a consensus sequence X3CGX7CX4CCSX2GXCGX5CX3CX3CX2 (Prosite PS50941), found in various plant and fungal defense proteins and is involved in the recognition and/or binding of chitin subunits (Finn et al. 2014).

To confirm carbohydrate binding, *E. coli* produced and Ni-NTA affinity purified recombinant VnaChtBP (e-Xtra Fig. S2) was used in a sedimentation assay with various carbohydrates. VnaChtBP bound specifically to chitin polymer, in the form of chitin beads and crab shell chitin, but not to the plant cell wall polymers cellulose and xylan (Fig. 3). To examine the affinity of VnaChtBP binding to chitin in more detail, recombinant protein was immobilized to the CM5 sensor chip and the VnaChtBP interaction with chitin hexamer was analyzed using surface plasmon resonance (SPR) (Kastritis and Bonvin 2013). VnaChtBP revealed concentration-dependent binding of chitin hexamer (Fig. 4) with a dissociation constant of 0.78 ± 0.58 µM, while no specific binding to other tested carbohydrates was detected (e-Xtra Fig. S3). Since the chitin binding affinity of the protein increases for longer chitin oligomers (Asensio et al. 2000), this value is comparable to other reported chitin oligomer binding affinities of fungal effectors but exceeds by one order of magnitude those reported for *Arabidopsis* chitin recognition receptors and hevein (Table 1). reported to protect fungal hyphae from plant chitinases (Van Den Burg et al. 2004; Marshall et al.

2011). To determine whether recombinant VnaChtBP can protect fungal cell walls against hydrolysis by plant chitinases, a cell protection assay adapted from Mentlak et al. (2012) was performed using germinating conidia of *Trichoderma viride*. Xylem sap extracted from *V. nonalfalfae* infected hop (Flajšman et al. 2018) was used as a source of plant chitinases. Chitinase activity was determined as a release of soluble Remazol brilliant violet 5R dye hydrolyzed from insoluble Chitin Azure substrate. The extracted xylem sap contained 19 U of active chitinase per mg of total protein. In the presence of xylem sap, only minimal germination of the *T. viride* conidia occurred after 24 h incubation, while pre-incubation in a 3 µM solution of recombinant VnaChtBP prior to the addition of xylem sap enabled germination of conidia and hyphal growth. Interestingly, aggregation and compaction of fungal hyphae were detected only in the presence of both xylem sap and VnaChtBP, while normal mycelial growth without hyphal aggregation was observed in the solution of VnaChtBP (Fig. 5). We assume that VnaChtBP, by binding and probably surrounding chitin fibers in the fungal cell wall, masks chitin and protects it from degradation by xylem sap chitinases.

VnaChtBP suppresses chitin-triggered plant immunity in hop

Several fungal chitin binding effectors prevent chitin mediated PTI trigger (Mentlak et al. 2012; Sanchez-Vallet et al. 2013; Takahara et al. 2016). To test whether VnaChtBP interferes with plant immune responses by sequestering chitin oligomers in the apoplast, the reactive oxygen species (ROS) released from the hop suspension cells in response to $(GlcNAc)_6$, in the presence or absence of VnaChtBP, were measured using a chemiluminescent assay. Treatment of hop suspension cells with 1 µM $(GlcNAc)_6$ resulted in a strong production of ROS, whereas this response was completely abolished in the presence of 5 µM VnaChtBP (Fig. 6).

It appears that similar to LysM effectors, CBM18-containing effector VnaChtBP can supress chitin-triggered generation of ROS and perturb plant immune responses.

VnaChtBP forms dimers and has two potential binding sites for interaction with chitin

Since many chitin binding proteins have been reported to form dimers (Liu et al. 2012; Sanchez-Vallet et al. 2013; Cao et al. 2014), a yeast-two-hybrid assay was carried out using *VnaChtBP* as both bait and prey to study the ability to dimerize. Dimer formation of VnaChtBP was detected on a minimal medium using histidine as a reporter (Fig. 7 A). Consistent with a weak interaction, only limited growth was observed on triple dropout reporter medium (synthetic complete medium without leucine, tryptophan and uracil) and the X-gal reporter was not activated. Far UV CD spectra of VnaChtBP in the presence and absence of chitin hexamer were obtained to show that binding of chitin to VnaChtBP induces additional secondary structure formation (Fig. 7 B). Based on the shape of the spectrum, the secondary structure is predominantly alpha helical.

To understand the chitin binding mechanism of CBM18 effectors better, homology modelling of the VnaChtBP 3D structure was performed. The SWISS-MODEL server produced three models based on different templates, shown in Table 2. Model02 provided the best fit for four out of six CBM18 modules and was used as the basis of the characterization. Molecular docking of the chitin hexamer into the VnaChtBP model (Fig. 7 C) shows that each protein monomer contributes to the formation of two

binding sites accessible to the ligand. In binding site I (BSI), chitin hexamer is accommodated in a shallow groove formed by four hevein domains of polypeptide chain A and two hevein domains of chain B, while binding site II (BSII) is comprised of four hevein domains of chain B and two domains of chain A. According to the analysis of the presented complex with YASARA, the binding of chitin hexamer in BSI is strengthened by eleven (four accepted and seven donated) hydrogen bonds and eight hydrophobic interactions, which contribute to the total binding energy of 6.891 kcal/mol (AutoDock/Vina) and an estimated docking score of 8.88 µM. A similar preference for binding of chitin hexamer in the BSII was observed, with an estimated docking score of 2.01 µM and a total binding energy of 7.772 kcal/mol, supported by eight (three accepted, five donated) hydrogen bonds and 12 hydrophobic interactions between the ligand and receptor.

VnaChtBP deletion has no significant effect on the growth and pathogenicity of *V. nonalfalfae*

Since *VnaChtBP* is specifically expressed during colonization of hop, its contribution to fungal virulence was tested in the susceptible hop variety 'Celeia'. *V. nonalfalfae* knockout mutants of *VnaChtBP* were generated by targeted gene disruption via *A. tumefaciens*-mediated transformation. Prior to plant inoculation, growth of fungal colonies and sporulation of knockout mutants were assessed *in vitro* and compared to the wild type (e-Xtra Fig. S4 A). In the selected knockout mutants, mycelial growth and fungal morphology did not differ significantly from the wild type. Reduced sporulation was observed for both mutants compared to the wild type but this did not impact on disease frequency. After inoculation of the hop plants, disease symptoms were independently assessed five times using a disease severity index (DSI) with a 0-5 scale (Radišek et al. 2003). After the final symptom assessment, the presence of fungus in all inoculated plants was confirmed through re-isolation tests. In addition, no differences in the relative amount of fungal DNA between the wild type and *VnaChtBP* mutant strains (e-Xtra Fig. S4 B) were observed on the basis of fungal biomass quantification in infected hop at 21 dpi.

Disease symptoms were monitored in susceptible hop following infection with the wild type *V. nonalfalfae* and knockout mutants of *VnaChtBP* (Fig. 8 A). Both *VnaChtBP* mutants displayed Verticillium wilting symptoms (chlorosis and necrosis of the leaves) in susceptible hop similar to the wild type fungus, with no significant differences among them according to the disease severity index (DSI) assessment (Fig. 8 B). Independent pathogenicity assays with additional *VnaChtBP* deletion mutants yielded the same results (data not shown). This suggests that the VnaChtBP function is redundant for *V. nonalfalfae* infection.

Discussion

V. nonalfalfae, a soil born fungal pathogen, causes serious economic damage in European hop growing regions. Significant efforts have been invested in studying the molecular mechanisms of Verticillium wilt in hop and fungus pathogenicity (Radišek et al. 2006; Jakše et al. 2013; Mandelc and Javornik 2015; Flajšman et al. 2016; Cregeen et al. 2015; Jakše et al. 2018; Marton et al. 2018).

In planta expressed fungal proteins are potential effector candidates that might be implicated in pathogen virulence. The effector candidate *V. nonalfalfae VnaChtBP* studied here, encodes for a CBM18

domain containing chitin binding protein and is highly expressed in hop plants. Using an established bioinformatic pipeline (Marton et al. 2018), we identified eleven genes in the *V. nonalfalfae* genome that contain CBM18 domains. Of these genes, two harboured a single CBM18 domain and five, including *VnaChtBP*, contain a predicted N-terminal signal peptide. Although CBMs play a key role in the recognition of carbohydrates and are known to promote efficient substrate hydrolysis as a part of carbohydrate-active enzymes (e.g., CBM18 motifs found in chitinases), they have also been found to be present in toxins, virulence factors and pathogenesis-associated proteins (Guillén et al. 2010). Proteins containing CBM18 motifs are common in fungi, particularly in plant and animal pathogens. Indeed, they are almost three times as common in the proteomes of pathogens than in those of non-pathogenic fungi across the phylum Ascomycota (Soanes et al. 2008). Intriguingly, in *Verticillium* spp., CBM18 containing genes are more frequently observed in mild pathogenic *V. tricorpus* (13) (Seidl et al. 2015) than in high pathogenic *V. dahliae* and *V. alfalfae* (9). The expansion of CBM18 domains in ChtBPs may be linked to the evolution of pathogenicity, and has, for example, been reported in the fungal pathogen *B. dendrobatidis*, which has caused a worldwide decline of amphibian populations (Abramyan and Stajich 2012). In total, eighteen genes with between one to eleven CBM18 domains have been identified in *B. dendrobatidis*, including some classified as lectin-like proteins. Biochemical characterization of three such lectin-like proteins revealed that two have a signal peptide and co-localize with chitinous cell wall in *Saccharomyces cerevisiae*. Furthermore, one of these proteins has been shown to bind chitin and thereby protect *Trichoderma reesei* from exogenous chitinase, suggesting a role of lectin-like proteins in fungal defence (Liu and Stajich 2015). Similarly, in the rice blast fungus *M. oryzae*, 15 genes with one to four CBM18 domains were found, although gene-targeted disruption and tolerance to chitinase treatment did not support the implication of the tested genes in fungal pathogenicity (Mochizuki et al. 2011).

VnaChtBP consists of six tandemly repeated CBM18 motifs, contains a signal peptide and is predicted to reside in the apoplast, which is consistent with the role of chitin binding in the extracellular space. Homology search of proteins that contain CBM18 motifs in other *Verticillium* species revealed that this type of protein is common in pathogenic *Verticillium* species but it seems not to be ubiquitous. For example, in the recently sequenced genomes of five *V. dahliae* strains isolated from strawberry, three strains harbored ChtBPs with five, six and ten CBM18 motifs, while none were detected in the two other strains.

Monitoring the *in planta* expression of *VnaChtBP* showed that it is highly expressed at the later stages of infection in a susceptible hop cultivar, and continues to be expressed even at 30 dpi, when plants exhibit severe wilting symptoms (Cregeen et al. 2015; Marton et al. 2018). In contrast, in a resistant cultivar, the *VnaChtBP* gene is slightly induced after infection and then completely down-regulated. The expression pattern of the *VnaChtBP* gene coincides with *V. nonalfalfae* colonization of hop, whereby the fungus spread is unimpeded in susceptible plants, while colonization is arrested around 12-20 dpi in resistant hop plants, presumably due to strong plant resistance responses (Cregeen et al. 2015). The immune reaction in the incompatible interaction is unlikely to impose selection pressure on the *VnaChtBP* gene since no allelic polymorphisms were detected among the analysed *V. nonalfalfae* isolates. Similarly, no allelic variation was found in the closest (97% identity) homolog to the *VnaChtBP* gene from isolates of *V.*

alfalfae, suggesting highly conserved genes. Allelic variation is commonly detected in fungal proteins that function as avirulent (Avr) determinants on perception by the host defence, but not necessarily in virulence factors of the pathogen (Stergiopoulos et al. 2007). Taken together, we speculate that the absence of allelic variation and the high gene expression observed *in planta* suggest a role for VnaChtBP in the virulence of *V. nonalfalfae*. However, in a pathogenicity assay, *VnaChtBP* targeted deletion mutants were not significantly impaired in their hops infectivity compared to wild type fungus which is in line with functional redundancy. Unchanged virulence of deletion mutants, presumably due to functional redundancy, has been reported for two other tested CBM18-containing ChtBPs in *M. oryzae* (Mochizuki et al. 2011) and also for LysM fungal effector, Mg1LysM, of *Mycosphaerella graminicola* (Marshall et al. 2011). Indeed, seven putative chitin binding LysM effectors have been found in the *V. nonalfalfae* genome, which may have a role in protection of the fungal cell wall chitin or may interfere with chitin-triggered plant immunity. Orthologues of *C. fulvum* Avr4 with the CBM14 chitin-binding motif were not identified in the *V. nonalfalfae* genome (Jakše et al. 2018) or in the predicted proteomes of other *Verticillium* species (Seidl et al. 2015).

Consistent with previously characterized CBM18 containing proteins from *M. oryzae* (Mochizuki et al. 2011) and *B. dendrobatidis* (Liu and Stajich 2015), recombinant VnaChtBP binds specifically to chitin beads and crab shell chitin, but not to plant cell wall cellulose or xylan. In addition to chitin polymer, recombinant VnaChtBP also bound chitin hexamer in an SPR experiment, with binding affinity in the submicromolar range. Compared to plant chitin receptors, recombinant VnaChtBP together with LysM effectors Ecp6 from *C. fulvum*, Slp1 from *M. oryzae* (Mentlak et al. 2012) and ChELP1 and ChELP2 from *C. higginsianum* (Takahara et al. 2016), exhibit three to five orders of magnitude higher affinity to chitin oligomers. It is thus not surprising that these fungal effectors are able to outcompete plant chitin receptors, such as *Arabidopsis thaliana* AtLYK5 (Cao et al. 2014) and AtCERK1 (Liu et al. 2012).

Based on NMR studies and solved crystal structures of plant LysM chitin receptors, several mechanisms for binding of chitin have been proposed; from a simple ‘continuous groove’ model for AtCERK1 (Liu et al. 2012) to the OsCEBiP ‘sandwich’ (Hayafune et al. 2014) and ‘sliding mode’ model (Liu et al. 2016). However, these models have been unable to explain the observed elicitor activities of chitin oligomers. Building on these models and using a range of chitosan polymers and oligomers bound to *Atcerk1* mutants resulted in an improved ‘slipped sandwich’ model that fits all experimental results (Gubaeva et al. 2018). A recent structural study of fungal LysM effector Ecp6 from *C. fulvum* revealed a novel chitin binding mechanism that explained how LysM effectors can outcompete plant host receptors for chitin binding (Sanchez-Vallet et al. 2013). Ecp6 consists of three tightly packed LysM domains, with a typical $\beta\alpha\alpha\beta$ fold. Intra-chain dimerization of chitin-binding regions of LysM1 and LysM3 leads to the formation of a deeply buried chitin binding groove with an ultra-high (pM) affinity. The remaining LysM2 domain also binds chitin, albeit with low micromolar affinity, and interferes with chitin-triggered immunity, possibly by preventing chitin immune receptor dimerization and not by chitin fragment sequestering, as in the case of LysM1-LysM3.

To date, to the best of our knowledge, the molecular mechanism of chitin binding of CBM18 fungal effectors remains elusive. However, the 3D homology model of VnaChtBP provides a tangible model for the molecular docking of the chitin hexamer. Although only four out of six CBM18 domains could be

reliably modelled, the analysis revealed that VnaChtBP dimerizes. Importantly, this prediction was independently validated through a yeast-two-hybrid experiment. The VnaChtBP complex has two putative chitin binding sites, which form a shallow binding cleft by cooperation of the two polypeptide chains and have a similar preference to chitin. As in CBM18 lectin-like plant defence proteins (Jiménez-Barbero et al. 2006), typically represented by a small antifungal protein hevein from the rubber tree (*Hevea brasiliensis*), a network of hydrogen bonds and several hydrophobic interactions occur between VnaChtBP residues and N-acetyl moieties of the chitin oligomer. These are thought to stabilize the interaction and contribute to submicromolar chitin binding affinity, as determined by CD and SPR experiments, respectively. Similarly, the recently solved crystal structure of fungal effector CfAvr4, a CBM14 lectin, in complex with chitin hexamer (Hurlburt et al. 2018), revealed that two effector molecules form a sandwich structure, which encloses two parallel stacked chitin hexamer molecules, shifted by one sugar ring, in an extended chitin binding site. In this complex, the interaction is mediated through aromatic residues and numerous hydrogen bonds, with both side chains and main chains. Interestingly, no intermolecular protein-protein interactions have been observed across the dimer, suggesting ligand induced effector dimerization.

Fungal plant pathogens have evolved several strategies to escape the surveillance of chitin-related immune systems (Sanchez-Vallet et al. 2014). The various mechanisms used include conversion of chitin to chitosan by chitin deacetylases and inclusion of α-1,3-glucan in the cell walls, as well as secretion of diverse effectors that can shield the fungal hyphae from hydrolysis by plant chitinases, directly inhibiting their activity, acting as scavengers of chitin fragments or preventing chitin–induced plant immunity. Suppression of chitin-triggered immunity has been demonstrated for some LysM effectors with subnanomolar affinity for chitin oligomers (Mentlak et al. 2012; Sanchez-Vallet et al. 2013; Takahara et al. 2016; Kombrink et al. 2017). Here, we find that VnaChtBP binds to chitin oligomers with submicromolar affinity, preventing free chitin oligomers from binding to plant immune receptors and thus suppressing ROS-related defense responses in hop. A protective role against host chitinases has been shown for secreted effector Avr4 from *C. fulvum*, which binds to fungal cell wall chitin to reduce its accessibility to host chitinases (van den Burg et al. 2007). Similar to CfAvr4, wheat pathogen *M. graminicola* secreted effectors Mg1LysM, Mg3LysM and *V. dahliae* effector Vd2LysM protect fungal hyphae from hydrolysis by plant chitinases (Marshall et al. 2011; Kombrink et al. 2017). We provide evidence that, in addition to Avr4 (CBM14) and LysM (CBM50) effectors, structurally unrelated CBM18 lectin-like proteins that are found in fungal pathogens of plants (this study) and amphibian pathogens (Liu and Stajich 2015) have evolved a chitin shielding ability against plant chitinases.

Materials and Methods

Cultivation of microorganisms

Escherichia coli MAX Efficiency DH5α or MAX Efficiency DH10B (both from Invitrogen, ThermoFisher Scientific) were used for plasmid propagation and were grown at 37°C on LB agar plates or liquid medium supplemented with appropriate antibiotics (carbenicillin 100 mg/liter, kanamycin 50 mg/liter or gentamicin 25 mg/liter). *E. coli* Shuffle T7 (New England Bioloabs) were propagated at 30°C and protein

expression was performed at 16°C. *Trichoderma viride* was obtained from The Microbial Culture Collection Ex (IC Mycosmo (MRIC UL)) and all *Verticillium* strains were from the Slovenian Institute of Hop Research and Brewing fungal collection. Fungi were grown at 24°C in the dark on ½ Czapek-Dox agar plates or liquid medium. Knockout mutants were retrieved from selection medium supplemented with 150 mg/liter timentin and 75 mg/liter hygromycin.

RNA sequencing

RNA-Seq library preparation from *V. nonalfalfae* infected hop at 6, 12, 18 and 30 days post inoculation (dpi) and data processing have been previously described (Progar et al. 2017). Fungal transcripts were filtered out and their gene expression profiles were generated using the Hierarchical clustering with Euclidean distance method in R language (R Core Team 2016). Data were presented as a matrix of log_2CPM (counts per million–number of reads mapped to a gene model per million reads mapped to the library) expression values.

VnaChtBP gene expression profiling with RT-qPCR

The expression of *VnaChtBP* was quantified by RT-qPCR in hop infected with *V. nonalfalfae* isolate T2. Total RNA was extracted at 6, 12, and 18 dpi using a Spectrum Plant total RNA kit (Sigma-Aldrich) and 1 µg was reverse transcribed to cDNA using a High Capacity cDNA reverse transcription kit (Applied Biosystems). The qPCR reaction was run in 5 biological and 2 technical replicates on an ABI PRISM 7500 (Applied Biosystems), under the following conditions: denaturation at 95°C for 10 min, followed by 40 cycles at 95°C for 10 s, 60°C for 30 s, and consisted of: 50 ng of cDNA, 300 nM forward and reverse primer, and 5 µl of Fast SYBR Green master mix (Roche). The results were analyzed using the $\Delta\Delta C_t$ method (Schmittgen and Livak 2008). Transcription levels of *VnaChtBP* were quantified relative to its expression in liquid Czapek-Dox medium and normalized to fungal biomass in hop using topoisomerase and splicing factor as reference genes (Marton et al. 2018). One way ANOVA with Tukey's post hoc test was performed to test for differences between the group means. Primers used are listed in e-Xtra Table S3.

Genetic analysis

Genomic DNA was extracted from 7-10 day PDA cultured *Verticillium* isolates by the CTAB extraction method (Möller et al. 1992). PCR reactions were performed in 50 µl using Q5® High-Fidelity DNA Polymerase (NEB), 500 nM gene-specific primers (e-Xtra Table S3) and 100 ng DNA under the following conditions: denaturation at 95°C for 10 min, followed by 40 cycles at 95°C for 10 s, 58°C for 30 s, 72°C for 90 s, and a final elongation step at 72°C for 90 s. PCR products were purified from agarose gel (Silica Bead DNA Gel Extraction Kit, Fermentas), cloned into pGEM®-T Easy vector (Promega) and sequenced using Sanger technology with gene-specific and plasmid-specific primers (e-Xtra Table S3). Sequences were analyzed using CodonCode Aligner V7.1.2 (CodonCode Co.) and deposited at the NCBI.

Bioinformatic analysis

A putative localization of VnaChtBP to the apoplast was predicted with ApoplastP 1.0 (Sperschneider et al. 2018). To classify *V. nonalfalfae* CBM18-containing proteins functionally, sequence based searches were carried out using the FunFHMMer web server at the CATH-Gene3D database (Dawson et al. 2017).

To obtain VnaChtBP homologs, the amino acid sequence of VnaChtBP was used as a query for NCBI BLAST+ against UniProt Knowledgebase at Interpro (Li et al. 2015).

Yeast-two-hybrid assay

Dimerization of VnaChtBP was examined with a yeast-two-hybrid experiment using the ProQuest Y2H system (Invitrogen). To generate bait and prey vectors, the *VnaChtBP* gene was cloned into pDEST22 and pDEST32, respectively, and co-transformed in yeast. The interactors were confirmed by plating the yeast co-transformants on triple dropout reporter medium SC-LWH (synthetic complete medium without leucine, tryptophan and histidine), on triple dropout reporter medium SC-LWU (synthetic complete medium without leucine, tryptophan and uracil) and by performing an X-gal assay. The self-activation test of a pDEST22 construct containing the *VnaChtBP* gene with empty pDEST32 vectors was also performed.

3D modelling and molecular docking

The SWISS-MODEL (Arnold et al. 2006; Waterhouse et al. 2018) server produced three models based on different templates and Model02 was selected for further modelling. The output protein structure was additionally minimized in explicit water using an AMBER14 force field (Duan et al. 2003) and 'em_runclean.mcr' script within YASARA Structure (Krieger and Vriend 2014, 2015). A 3D structure model of chitin hexamer was built with SWEET PROGRAM v.2 (Bohne et al. 1998, 1999), saved as a PDB file and used as a ligand in subsequent molecular docking experiments with AUTODOCK/VINA (Trott and Olson 2010), which is incorporated into YASARA Structure. To ensure the integrity of docking results, 200 independent dockings of the ligand to the receptor were performed. The pose with the best docking score was selected for further refinement using 'md_refine.mcr' script provided by YASARA Structure. The final model of the hexameric chitin bound to the VnaChtBP dimer was then used for the analysis.

Recombinant protein production

VnaChtBP DNA without predicted signal peptide (SignalP 4.1) was cloned into a pET32a expression vector using a Gibson Assembly® Cloning Kit (NEB). The protein expression in *E. coli* SHuffle® T7 cells (NEB) was induced at OD_{600} = 0.6 with 1 mM IPTG and incubated overnight at 16°C. The recombinant protein was solubilized from inclusion bodies using a mild solubilization method (Qi et al. 2015). Briefly, pelleted cells were resuspended in cold PBS buffer and disrupted by sonication. After centrifugation, the pellet was washed with PBS, resuspended in urea, frozen at -20°C and allowed to slowly thaw at RT. The recombinant protein was purified using Ni-NTA Spin Columns (Qiagen) according to the manufacturer's protocol, aliquoted and stored in 20 mM Tris (pH 8.0) at -80°C.

Carbohydrate sedimentation assay and Western blot detection

The carbohydrate sedimentation assay was adapted from (van den Burg et al. 2007). Briefly, 15 µg of recombinant VnaChtBP in 20 mM Tris (pH 8.0) was mixed with 1.5 mg of chitin magnetic beads (NEB), crab shell chitin (Sigma-Aldrich), cellulose (Sigma-Aldrich) or xylan (Apollo Scientific) and incubated at RT for 2 h on an orbital shaker at 350 rpm. The same amount of protein in Tris buffer without added carbohydrates was used as a negative control. After centrifugation (5 min, 13,000 g), the supernatant was collected and the pellet was washed three times with 800 µl 20 mM Tris (pH 8.0) prior to resuspension in 4X Bolt™ LDS Sample Buffer with the addition of reducing agent (Invitrogen).

The presence of VnaChtBP in different fractions was determined by WB analysis. Samples (25 µL) were loaded on a precast Bolt™ 4-12% Bis-Tris gel (Invitrogen) and SDS-PAGE in 1x MOPS running buffer was performed using a Mini Gel Tank (ThermoFisher Scientific) for 30 min at 200 V. Proteins were transferred for 1 h at 30 V to an Invitrolon PVDF membrane (Invitrogen) and Ponceau S stained. The membrane was blocked with 5% BSA in 1x PBS before the addition of the primary antibody His-probe (H-3) (SCBT) (1:1,000). The membrane was incubated overnight at 4°C, washed with 1x PBS and incubated in a solution of secondary Chicken anti-mouse IgG-HRP (SCBT) (1:5,000) for 1 h. Protein bands were detected using Super Signal West Pico (ThermoFisher Scientific) ECL substrate in a GelDoc-It2 Imager (UVP).

Surface plasmon resonance

The binding of hexa-N-acetyl chitohexaose ($(GlcNAc)_6$; IsoSep) to VnaChtBP was measured using a Biacore T100 analytical system and CM5 sensor chip (Biacore, GE Healthcare). The CM5 sensor chip was activated using an Amine coupling Kit (GE Healthcare) according to the manufacturer's instructions. VnaChtBP was diluted into 10 mM sodium acetate pH 5.1 to a final concentration of 0.1 mg/ml and injected for five minutes over the second flow cell. The first flow cell was empty and served as a reference cell to control the level of non-specific binding. The final immobilization level was approximately 10,000 response units (RU). The $(GlcNAc)_6$ stock solution was diluted into a series of concentrations (0.05, 0.1, 0.2, 0.4, 0.8, 1.6, 3.2 and 6.4 µM) with HBS buffer (10 mM HEPES, 140 mM NaCl, pH 7.4) and assayed to detect direct binding to VnaChtBP. Titration was performed in triplicate. In addition to chitin hexamer, N-acetyl glucosamine, glucosamine, glucose, galactose and mannose were tested at a 500 µM concentration in HBS buffer. Biacore T100 Evaluation software was used to assess the results. First, the sensorgrams were reference and blank subtracted, then a Steady State Affinity model was applied to calculate the affinity constant (K_d). The average of three repeated experiments was used for final K_d determination.

Circular dichroism

Far UV CD spectra were recorded on a Jasco J-1500 CD spectrometer from 190 to 260 nm at 25 °C using a 0.1 cm path length quartz cuvette. The VnaChtBP concentration in 20 mM Tris (pH 8.0) was 2.5 µM and hexa-N-acetyl chitohexaose ($(GlcNAc)_6$, Santa Cruz Biotechnology) was at 25 µM final concentration. Measurements were performed at a 1 nm interval and 5 nm/min scanning speed by using a 1 nm bandwidth. Final spectra were baseline-corrected and transformed to mean residue ellipticity using a mean residue weight of VnaChtBP of 99.851 Da.

Xylem sap extraction and chitinase activity assay

Xylem sap was extracted from infected hop plants in a pressure chamber at 0.2 MPa for 120 min (Flajšman et al. 2018). The chitinase activity of xylem sap was determined by mixing 150 µl of xylem sap, or 100 mM Na-acetate (pH 5.0) buffer as negative control, with 1.5 mg of Chitin Azure (Sigma-Aldrich) dissolved in 150 µl 100 mM Na-acetate (pH 5.0). The samples were incubated for 150 min at 25°C on a rotary shaker at 70 rpm. An aliquot of 80 µl was taken immediately (blank sample) and after 150 min. The reaction was stopped with the addition of 20%v/v HCl and samples were centrifuged for 10 min at 10,000 g. The chitinase activity of xylem sap in the supernatant was determined by measuring the absorbance of released Remazol Brilliant Blue dye at 575 nm against 100 mM Na-acetate (pH 5.0). One

enzyme unit was defined as the amount of chitinase that produced a 0.01 increase in absorbance at 575 nm, measured at 25°C and pH 5.0. The total protein concentration of the xylem sap was measured in a 10x diluted sample using a Pierce™ BCA Protein Assay Kit (Thermo Scientific) following the standard protocol.

Cell Protection Assay

The cell protection assay was adapted from Mentlak et al., 2012. *Trichoderma viride* conidia were harvested, diluted to 2,000 conidia/ml in 50 µl ½ Czapek-dox medium and incubated overnight. After germination of the conidia, 25 µl of recombinant VnaChtBP (3 µM final concentration) or an equal volume of storage buffer (20 mM Tris; pH 8.0) were added and the conidial suspensions were incubated for 2 h. Fungal cell wall hydrolysis was triggered by the addition of 25 µl of xylem sap as a source of plant chitinases, while 25 µl of Na-acetate (100 mM; pH 5.0) was used in the control experiment. After 24 h incubation, mycelia formation and fungal growth were examined using a Nikon Eclipse 600 microscope.

Reactive oxygen species production

Hop suspension cells were prepared from hop tissue culture (obtained from the Slovenian Institute of Hop Research and Brewing) as described previously (Langezaal and Scheffer 1992). Briefly, the internodal segments were cultured on solid MS media supplemented with 1 mg/l 2,4-D and 1 mg/l kinetin and calluses were subcultured every two weeks. For initiation of suspension cell culture, 5 g of fresh callus were resuspended in 50 ml of liquid MS media, grown in the dark at 140 rpm and then maintained by subculturing every two weeks.

One week old hop suspension cells were harvested by centrifugation and MS medium was replaced by sterile distilled water prior to ROS measurements. For each treatment, a 150 µl aliquot of suspension cells was mixed with a 150 µl assay solution, containing 100 µM L-012 substrate (Sigma, USA), 40 µg/ml horseradish peroxidase (Sigma, USA) and either 1 µM chitin ($(GlcNAc)_6$, Santa Cruz Biotechnology), 5 µM VnaChtBP, a combination of 1 µM chitin ($(GlcNAc)_6$ and 5 µM VnaChtBP, or sterile distilled water as negative control. Luminol-based chemiluminescence measurements were recorded for 30 min at a minimal interval (of 2 min 5 s) in a Synergy H1 microplate reader (BioTek Instruments). Data were baseline-corrected and presented as a median with 95% confidence interval of 5 measurements. R package DescTools (Signorell 2017) was used to calculate the area under the curve. A non-parametric Kruskal-Wallis test with Holm's post hoc analysis was used to test the differences between the chitin-treated group, VnaChtBP-treated group and the chitin plus VnaChtBP group.

Pathogenicity assay

VnaChtBP knockout mutants were generated using the *Agrobacterium tumefaciens* mediated transformation protocol described previously (Flajšman et al. 2016) and primers listed in e-Xtra Table S3. Before the pathogenicity tests were carried out, fungal growth and sporulation were inspected as described previously (Flajšman et al. 2017). Briefly, sporulation of fungal samples from liquid Czapek-Dox medium was assessed using a Thoma cell counting chamber under a light microscope. Wild type strain T2 was attributed grade 5 – indicating 100% sporulation (typically reaching 10^7 spores per ml after 1 week). Sporulation of mutant strains was then compared to that of the wild type on a scale from 0-5, with a 20% interval.

For the pathogenicity assay, ten plants of the Verticillium wilt susceptible hop cultivar 'Celeia' were inoculated by 10-min root dipping in a conidia suspension (5× 10^6 conidia/ml) of two arbitrarily selected *VnaChtBP* knockout mutants. Conidia of the wild type *V. nonalfalfae* isolate T2 served as a positive control and sterile distilled water was used as a mock control. Re-potted plants were grown under controlled conditions in a growth chamber (Flajšman et al. 2017). Verticillium wilting symptoms were assessed five times over seven weeks post-inoculation using a disease severity index (DSI) with a 0-5 scale (Radišek et al. 2003). After symptom assessment, a fungal re-isolation test (Flajšman et al. 2017) was performed to confirm infection of the tested hop plants.

In addition, fungal biomass quantification was carried out in five hop plants infected with either wild type or *VnaChtBP* mutant *V. nonalfalfae* strains. Samples were collected at 21 dpi and total genomic DNA was extracted using the CTAB protocol (Möller et al. 1992). Fungal DNA was quantified on the Applied Biosystems® 7500 real-time quantitative PCR system (Applied Biosystems) using Fast SYBR® Green technology (Thermo Fisher Scientific) and *V. nonalfalfae* lethal genotype (PG2) specific primer 5-1gs (Radišek et al. 2004). The relative quantity of *V. nonalfalfae* DNA in infected hop was estimated with the $2^{-\Delta\Delta Ct}$ method (Schmittgen and Livak 2008) using the hop reference gene DRH1 (DEAD box RNA helicase) for normalization (Štajner et al. 2013). One-way ANOVA with Tukey's multiple comparison test was performed in GraphPad Prism 8.02 (GraphPad Software, San Diego, California USA, www.graphpad.com) to test for differences between the wild type and mutant group means.

Acknowledgments

This research was supported by the Slovenian Research Agency grants P4-0077, J4-8220 and fellowship 342257. This work benefitted from interactions promoted by the COST Action FA 1208 https://cost-sustain.org. The authors would like to thank Dr Vasja Progar for transcriptome analysis, Dr Vesna Hodnik for SPR analysis and Dr Miles Armstrong, Miha Bahun, Urban Kunej, Dr Marko Dolinar, Dr Jernej Jakše and Dr Nataša Poklar Ulrih for technical advice.

Literature Cited

Abramyan, J., and Stajich, J. E. 2012. Species-specific chitin-binding module 18 expansion in the amphibian pathogen Batrachochytrium dendrobatidis. MBio. 3:e00150-12

Akcapinar, G. B., Kappel, L., Sezerman, O. U., and Seidl-Seiboth, V. 2015. Molecular diversity of LysM carbohydrate-binding motifs in fungi. Curr. Genet. 61:103–113

Andersen, N. H., Cao, B., Rodríguez-Romero, A., and Arreguin, B. 1993. Hevein: NMR Assignment and Assessment of Solution-State Folding for the Agglutinin-Toxin Motif. Biochemistry. 32:1407–1422

Arnold, K., Bordoli, L., Kopp, J., and Schwede, T. 2006. The SWISS-MODEL workspace: a web-based environment for protein structure homology modelling. Bioinformatics. 22:195–201

Asensio, J. L., Cañada, F. J., Siebert, H.-C., Laynez, J., Poveda, A., Nieto, P. M., Soedjanaamadja, U., Gabius, H.-J., and Jiménez-Barbero, J. 2000. Structural basis for chitin recognition by defense proteins: GlcNAc residues are bound in a multivalent fashion by extended binding sites in hevein

domains. Chem. Biol. 7:529–543

Böhm, H., Albert, I., Fan, L., Reinhard, A. A., and Nürnberger, T. 2014. Immune receptor complexes at the plant cell surface. Curr. Opin. Plant Biol. 20:47–54

Bohne, A., Lang, E., and von der Lieth, C.-W. 1998. W3-SWEET: Carbohydrate Modeling By Internet. J. Mol. Model. 4:33–43

Bohne, A., Lang, E., and von der Lieth, C. W. 1999. SWEET - WWW-based rapid 3D construction of oligo- and polysaccharides. Bioinformatics. 15:767–768

Boller, T., and Felix, G. 2009. A renaissance of elicitors: perception of microbe-associated molecular patterns and danger signals by pattern-recognition receptors. Annu. Rev. Plant Biol. 60:379–406

Bolton, M. D., Van Esse, H. P., Vossen, J. H., De Jonge, R., Stergiopoulos, I., Stulemeijer, I. J. E., Van Den Berg, G. C. M., Borrás-Hidalgo, O., Dekker, H. L., De Koster, C. G., De Wit, P. J. G. M., Joosten, M. H. A. J., and Thomma, B. P. H. J. 2008. The novel Cladosporium fulvum lysin motif effector Ecp6 is a virulence factor with orthologues in other fungal species. Mol. Microbiol. 69:119–136

van den Burg, H. A., Harrison, S. J., Joosten, M. H. A. J., Vervoort, J., and de Wit, P. J. G. M. 2007. Cladosporium fulvum Avr4 Protects Fungal Cell Walls Against Hydrolysis by Plant Chitinases Accumulating During Infection. Mol. Plant-Microbe Interact. 19:1420–1430

Van Den Burg, H. A., Spronk, C. A. E. M., Boeren, S., Kennedy, M. A., Vissers, J. P. C., Vuister, G. W., De Wit, P. J. G. M., and Vervoort, J. 2004. Binding of the AVR4 elicitor of Cladosporium fulvum to chitotriose units is facilitated by positive allosteric protein-protein interactions: The chitin-binding site of AVR4 represents a novel binding site on the folding scaffold shared between the inverte. J. Biol. Chem. 279:16786–16796

Cao, Y., Liang, Y., Tanaka, K., Nguyen, C. T., Jedrzejczak, R. P., Joachimiak, A., and Stacey, G. 2014. The kinase LYK5 is a major chitin receptor in Arabidopsis and forms a chitin-induced complex with related kinase CERK1. Elife. 3

Cregeen, S., Radišek, S., Mandelc, S., Turk, B., Štajner, N., Jakše, J., and Javornik, B. 2015. Different Gene Expressions of Resistant and Susceptible Hop Cultivars in Response to Infection with a Highly Aggressive Strain of Verticillium albo-atrum. Plant Mol. Biol. Report. 33:689–704

Dawson, N. L., Sillitoe, I., Lees, J. G., Lam, S. D., and Orengo, C. A. 2017. CATH-Gene3D: Generation of the resource and its use in obtaining structural and functional annotations for protein sequences. Pages 79–110 in: Protein Bioinformatics. Methods in Molecular Biology

Dodds, P. N., and Rathjen, J. P. 2010. Plant immunity: Towards an integrated view of plantĝ€" pathogen interactions. Nat. Rev. Genet. 11:539–548

Duan, Y., Wu, C., Chowdhury, S., Lee, M. C., Xiong, G., Zhang, W., Yang, R., Cieplak, P., Luo, R., Lee, T., Caldwell, J., Wang, J., and Kollman, P. 2003. A point-charge force field for molecular mechanics simulations of proteins based on condensed-phase quantum mechanical calculations. J. Comput. Chem. 24:1999–2012

van Esse, H. P., Bolton, M. D., Stergiopoulos, I., de Wit, P. J. G. M., and Thomma, B. P. H. J. 2007. The Chitin-Binding Cladosporium fulvum Effector Protein Avr4 Is a Virulence Factor. Mol. Plant-Microbe

609 Interact. 20:1092–1101

610 Finn, R. D., Bateman, A., Clements, J., Coggill, P., Eberhardt, R. Y., Eddy, S. R., Heger, A., Hetherington, K.,
611 Holm, L., Mistry, J., Sonnhammer, E. L. L., Tate, J., and Punta, M. 2014. Pfam: The protein families
612 database. Nucleic Acids Res. 42:222–230

613 Flajšman, M., Mandelc, S., Radišek, S., and Javornik, B. 2018. Xylem Sap Extraction Method from Hop
614 Plants. BIO-PROTOCOL. 7:1–11

615 Flajšman, M., Mandelc, S., Radišek, S., Štajner, N. N., Jakše, J., Košmelj, K., and Javornik, B. 2016.
616 Identification of Novel Virulence-Associated Proteins Secreted to Xylem by Verticillium nonalfalfae
617 During Colonization of Hop Plants. 29:362–373

618 Flajšman, M., Radišek, S., and Javornik, B. 2017. Pathogenicity Assay of Verticillium nonalfalfae on Hop
619 Plants. BIO-PROTOCOL. 7:1–10

620 Gubaeva, E., Gubaev, A., Melcher, R. L. J., Cord-Landwehr, S., Singh, R., El Gueddari, N. E., and
621 Moerschbacher, B. M. 2018. 'Slipped Sandwich' Model for Chitin and Chitosan Perception in
622 Arabidopsis. Mol. Plant-Microbe Interact. 31:1145–1153

623 Guillén, D., Sánchez, S., and Rodríguez-Sanoja, R. 2010. Carbohydrate-binding domains: multiplicity of
624 biological roles. Appl. Microbiol. Biotechnol. 85:1241–1249

625 Gust, A. A., Willmann, R., Desaki, Y., Grabherr, H. M., and Nürnberger, T. 2012. Plant LysM proteins:
626 modules mediating symbiosis and immunity. Trends Plant Sci. 17:495–502

627 Hayafune, M., Berisio, R., Marchetti, R., Silipo, A., Kayama, M., Desaki, Y., Arima, S., Squeglia, F.,
628 Ruggiero, A., Tokuyasu, K., Molinaro, A., Kaku, H., and Shibuya, N. 2014. Chitin-induced activation of
629 immune signaling by the rice receptor CEBiP relies on a unique sandwich-type dimerization. Proc.
630 Natl. Acad. Sci. 111:E404–E413

631 Hurlburt, N. K., Chen, L.-H., Stergiopoulos, I., and Fisher, A. J. 2018. Structure of the Cladosporium fulvum
632 Avr4 effector in complex with (GlcNAc)6 reveals the ligand-binding mechanism and uncouples its
633 intrinsic function from recognition by the Cf-4 resistance protein Y. Wang, ed. PLOS Pathog.
634 14:e1007263

635 Jakše, J., Čerenak, A., Radišek, S., Satovic, Z., Luthar, Z., and Javornik, B. 2013. Identification of
636 quantitative trait loci for resistance to Verticillium wilt and yield parameters in hop (Humulus
637 lupulus L.). Theor. Appl. Genet. 126:1431–1443

638 Jakše, J., Jelen, V., Radišek, S., de Jonge, R., Mandelc, S., Majer, A., Curk, T., Zupan, B., Thomma, B. P. H.
639 J., and Javornik, B. 2018. Genome sequence of xylem-invading Verticillium nonalfalfae lethal strain.
640 Genome Announc. 6:e01458-17

641 Jiménez-Barbero, J., Javier Cañada, F., Asensio, J. L., Aboitiz, N., Vidal, P., Canales, A., Groves, P., Gabius,
642 H.-J., and Siebert, H.-C. 2006. Hevein Domains: An Attractive Model to Study Carbohydrate–Protein
643 Interactions at Atomic Resolution. Adv. Carbohydr. Chem. Biochem. 60:303–354

644 Jones, J. D. G. G., and Dangl, J. L. 2006. The plant immune system. Nature. 444:323–329

645 de Jonge, R., van Esse, H. P., Kombrink, A., Shinya, T., Desaki, Y., Bours, R., van der Krol, S., Shibuya, N.,
646 Joosten, M. H. A. J., and Thomma, B. P. H. J. 2010. Conserved fungal LysM effector Ecp6 prevents

chitin-triggered immunity in plants. Science. 329:953–955

de Jonge, R., and Thomma, B. P. H. J. 2009. Fungal LysM effectors: extinguishers of host immunity? Trends Microbiol. 17:151–157

Kastritis, P. L., and Bonvin, A. M. J. J. 2013. On the binding affinity of macromolecular interactions: Daring to ask why proteins interact. J. R. Soc. Interface. 10:20120835

Kombrink, A., Rovenich, H., Shi-Kunne, X., Rojas-Padilla, E., van den Berg, G. C. M., Domazakis, E., de Jonge, R., Valkenburg, D. J., Sanchez-Vallet, A., Seidl, M. F., and Thomma, B. P. H. J. 2017. Verticillium dahliae LysM effectors differentially contribute to virulence on plant hosts. Mol. Plant Pathol. 18:596–608

Krieger, E., and Vriend, G. 2015. New ways to boost molecular dynamics simulations. J. Comput. Chem. 36:996–1007

Krieger, E., and Vriend, G. 2014. YASARA View - molecular graphics for all devices - from smartphones to workstations. Bioinformatics. 30:2981–2982

Langezaal, C. R., and Scheffer, J. J. C. 1992. Initiation and growth characterization of some hop cell suspension cultures. Plant Cell. Tissue Organ Cult. 30:159–164

Lerner, D. R., and Raikhel, N. V. 1992. The gene for stinging nettle lectin (Urtica dioica agglutinin) encodes both a lectin and a chitinase. J. Biol. Chem. 267:11085–11091

Li, W., Cowley, A., Uludag, M., Gur, T., McWilliam, H., Squizzato, S., Park, Y. M., Buso, N., and Lopez, R. 2015. The EMBL-EBI bioinformatics web and programmatic tools framework. Nucleic Acids Res. 43:W580–W584

Liu, P., and Stajich, J. E. 2015. Characterization of the Carbohydrate Binding Module 18 gene family in the amphibian pathogen Batrachochytrium dendrobatidis. Fungal Genet. Biol. 77:31–39

Liu, S., Wang, J., Han, Z., Gong, X., Zhang, H., and Chai, J. 2016. Molecular Mechanism for Fungal Cell Wall Recognition by Rice Chitin Receptor OsCEBiP. Structure. 24:1192–1200

Liu, T., Liu, Z., Song, C., Hu, Y., Han, Z., She, J., Fan, G., Wang, J., Jin, C., Chang, J., Zhou, J. M., and Chai, J. 2012. Chitin-induced dimerization activates a plant immune receptor. Science. 336:1160–1164

Liu, W., Xie, Y., Ma, J., Luo, X., Nie, P., Zuo, Z., Lahrmann, U., Zhao, Q., Zheng, Y., Zhao, Y., Xue, Y., and Ren, J. 2015. IBS: an illustrator for the presentation and visualization of biological sequences. Bioinformatics. 31:3359–61

Lombard, V., Golaconda Ramulu, H., Drula, E., Coutinho, P. M., and Henrissat, B. 2014. The carbohydrate-active enzymes database (CAZy) in 2013. Nucleic Acids Res. 42:D490-495

Macho, A. P., and Zipfel, C. 2014. Plant PRRs and the activation of innate immune signaling. Mol. Cell. 54:263–272

Mandelc, S., and Javornik, B. 2015. The secretome of vascular wilt pathogen Verticillium albo-atrum in simulated xylem fluid. Proteomics. 15:787–797

Marshall, R., Kombrink, A., Motteram, J., Loza-Reyes, E., Lucas, J., Hammond-Kosack, K. E., Thomma, B. P.

683 H. J., and Rudd, J. J. 2011. Analysis of Two in Planta Expressed LysM Effector Homologs from the
684 Fungus Mycosphaerella graminicola Reveals Novel Functional Properties and Varying Contributions
685 to Virulence on Wheat. PLANT Physiol. 156:756–769

686 Marton, K., Flajšman, M., Radišek, S., Košmelj, K., Jakše, J., Javornik, B., and Berne, S. 2018.
687 Comprehensive analysis of Verticillium nonalfalfae in silico secretome uncovers putative effector
688 proteins expressed during hop invasion. PLoS One. 13:e0198971

689 Mentlak, T., Kombrink, A., Shinya, T., Ryder, L. S., Otomo, I., Saitoh, H., Terauchi, R., Nishizawa, Y.,
690 Shibuya, N., Thomma, B. P. H. J., and Talbot, N. J. 2012. Effector-Mediated Suppression of Chitin-
691 Triggered Immunity by Magnaporthe oryzae Is Necessary for Rice Blast Disease. Plant Cell. 24:322–
692 335

693 Miya, A., Albert, P., Shinya, T., Desaki, Y., Ichimura, K., Shirasu, K., Narusaka, Y., Kawakami, N., Kaku, H.,
694 and Shibuya, N. 2007. CERK1, a LysM receptor kinase, is essential for chitin elicitor signaling in
695 Arabidopsis. Proc. Natl. Acad. Sci. 104:19613–19618

696 Mochizuki, S., Saitoh, K. ichiro, Minami, E., and Nishizawa, Y. 2011. Localization of probe-accessible chitin
697 and characterization of genes encoding chitin-binding domains during rice-Magnaporthe oryzae
698 interactions. J. Gen. Plant Pathol. 77:163–173

699 Möller, E. M. M., Bahnweg, G., Sandermann, H., and Geiger, H. H. H. 1992. A simple and efficient
700 protocol for isolation of high molecular weight DNA from filamentous fungi, fruit bodies, and
701 infected plant tissues. Nucleic Acids Res. 20:6115–6116

702 Progar, V., Jakše, J., Štajner, N., Radišek, S., Javornik, B., and Berne, S. 2017. Comparative transcriptional
703 analysis of hop responses to infection with Verticillium nonalfalfae. Plant Cell Rep. 36:1599–1613

704 Punja, Z. K., and Zhang, Y.-Y. 1993. Plant chitinases and their roles in resistance to fungal diseases. J.
705 Nematol. 25:526–540

706 Pusztahelyi, T. 2018. Chitin and chitin-related compounds in plant-fungal interactions. Mycology. 9:189–
707 201

708 Qi, X., Sun, Y., and Xiong, S. 2015. A single freeze-thawing cycle for highly efficient solubilization of
709 inclusion body proteins and its refolding into bioactive form. Microb. Cell Fact. 14:1–12

710 R Core Team. 2016. R: A Language and Environment for Statistical Computing.

711 Radišek, S., Jakše, J., and Javornik, B. 2004. Development of pathotype-specific SCAR markers for
712 detection of Verticillium albo-atrum isolates from hop. Plant Dis. 88:1115–1122

713 Radišek, S., Jakše, J., and Javornik, B. 2006. Genetic variability and virulence among Verticillium albo-
714 atrum isolates from hop. Eur. J. Plant Pathol. 116:301–314

715 Radišek, S., Jakše, J., Simončič, A., and Javornik, B. B. 2003. Characterization of Verticillium albo-atrum
716 Field Isolates Using Pathogenicity Data and AFLP Analysis. Plant Dis. 87:633–638

717 Ranf, S. 2017. Sensing of molecular patterns through cell surface immune receptors. Curr. Opin. Plant
718 Biol. 38:68–77

719 Sanchez-Vallet, A., Mesters, J. R., and Thomma, B. P. H. J. 2014. The battle for chitin recognition in plant-

720 microbe interactions. FEMS Microbiol. Rev. 39:171–183

721 Sanchez-Vallet, A., Saleem-Batcha, R., Kombrink, A., Hansen, G., Valkenburg, D.-J. J., Thomma, B. P. H. J.,
722 and Mesters, J. R. 2013. Fungal effector Ecp6 outcompetes host immune receptor for chitin binding
723 through intrachain LysM dimerization. Elife. 2013:1–16

724 Schmittgen, T. D., and Livak, K. J. 2008. Analyzing real-time PCR data by the comparative C(T) method.
725 Nat. Protoc. 3:1101–1108

726 Seidl, M. F., Faino, L., Shi-Kunne, X., van den Berg, G. C. M., Bolton, M. D., and Thomma, B. P. H. J. 2015.
727 The Genome of the Saprophytic Fungus *Verticillium tricorpus* Reveals a Complex Effector Repertoire
728 Resembling That of Its Pathogenic Relatives. Mol. Plant-Microbe Interact. 28:362–373

729 Shibuya, N., and Minami, E. 2001. Oligosaccharide signalling for defence responses in plant. Physiol. Mol.
730 Plant Pathol. 59:223–233

731 Shimizu, T., Nakano, T., Takamizawa, D., Desaki, Y., Ishii-Minami, N., Nishizawa, Y., Minami, E., Okada, K.,
732 Yamane, H., Kaku, H., and Shibuya, N. 2010. Two LysM receptor molecules, CEBiP and OsCERK1,
733 cooperatively regulate chitin elicitor signaling in rice. Plant J. 64:204–214

734 Shinya, T., Nakagawa, T., Kaku, H., and Shibuya, N. 2015. Chitin-mediated plant–fungal interactions:
735 catching, hiding and handshaking. Curr. Opin. Plant Biol. 26:64–71

736 Signorell, A. 2017. DescTools v0.99.19. Available at:
737 https://www.rdocumentation.org/packages/DescTools/versions/0.99.19.

738 Soanes, D. M., Alam, I., Cornell, M., Wong, H. M., Hedeler, C., Paton, N. W., Rattray, M., Hubbard, S. J.,
739 Oliver, S. G., and Talbot, N. J. 2008. Comparative genome analysis of filamentous fungi reveals gene
740 family expansions associated with fungal pathogenesis. PLoS One. 3:e2300

741 Sperschneider, J., Dodds, P. N., Singh, K. B., and Taylor, J. M. 2018. ApoplastP: prediction of effectors and
742 plant proteins in the apoplast using machine learning. New Phytol. 217:1764–1778

743 Štajner, N., Cregeen, S., and Javornik, B. 2013. Evaluation of Reference Genes for RT-qPCR Expression
744 Studies in Hop (Humulus lupulus L.) during Infection with Vascular Pathogen Verticillium albo-
745 atrum. PLoS One. 8:e68228

746 Stergiopoulos, I., van den Burg, H. A., Okmen, B., Beenen, H. G., van Liere, S., Kema, G. H. J., and de Wit,
747 P. J. G. M. 2010. Tomato Cf resistance proteins mediate recognition of cognate homologous
748 effectors from fungi pathogenic on dicots and monocots. Proc. Natl. Acad. Sci. 107:7610–7615

749 Stergiopoulos, I., De Kock, M. J. D., Lindhout, P., and De Wit, P. J. G. M. 2007. Allelic variation in the
750 effector genes of the tomato pathogen Cladosporium fulvum reveals different modes of adaptive
751 evolution. Mol. Plant. Microbe. Interact. 20:1271–1283

752 Takahara, H., Hacquard, S., Kombrink, A., Hughes, H. B., Halder, V., Robin, G. P., Hiruma, K., Neumann, U.,
753 Shinya, T., Kombrink, E., Shibuya, N., Thomma, B. P. H. J., O'Connell, R. J., and Connell, R. J. O. 2016.
754 Colletotrichum higginsianum extracellular LysM proteins play dual roles in appressorial function
755 and suppression of chitin-triggered plant immunity. New Phytol. 211:1323–1337

756 Trott, O., and Olson, A. J. 2010. Software news and update AutoDock Vina: Improving the speed and
757 accuracy of docking with a new scoring function, efficient optimization, and multithreading. J.

758 Comput. Chem. 31:455–461

759 Waterhouse, A., Bertoni, M., Bienert, S., Studer, G., Tauriello, G., Gumienny, R., Heer, F. T., de Beer, T. A.
760 P., Rempfer, C., Bordoli, L., Lepore, R., and Schwede, T. 2018. SWISS-MODEL: homology modelling
761 of protein structures and complexes. Nucleic Acids Res. 46:W296–W303

762 Wright, H. T., Sandrasegaram, G., and Wright, C. S. 1991. Evolution of a family of N-acetylglucosamine
763 binding proteins containing the disulfide-rich domain of wheat germ agglutinin. J. Mol. Evol.
764 33:283–294

765

Tables

Table 1. Comparison of chitin oligomer binding affinities of various fungal effectors and plant defense proteins, obtained using ITC or SPR. The proteins are organized according to binding affinity.

Organism	Protein	CAZy	Ligand	K_d (µM)	Method	Reference
FUNGUS						
Cladosporium fulvum	Ecp6	CBM50	$(GlcNAc)_6$	2.8 x 10^{-4}, [a] 1.7	ITC	(Sanchez-Vallet et al. 2013)
Colletotrichum higginsianum	ChELP1	CBM50	$(GlcNAc)_8$-Bio	2.6 x 10^{-5}	SPR	(Takahara et al. 2016)
Colletotrichum higginsianum	ChELP2	CBM50	$(GlcNAc)_8$-Bio	2.5 x 10^{-4}	SPR	(Takahara et al. 2016)
Cladosporium fulvum	Ecp6	CBM50	$(GlcNAc)_8$	1.3 x 10^{-3}	SPR	(Mentlak et al. 2012)
Magnaporthe oryzae	Slp1	CBM50	$(GlcNAc)_8$	2.4 x 10^{-3}	SPR	(Mentlak et al. 2012)
Verticillium nonalfalfae	VnaChtBP	CBM18	$(GlcNAc)_6$	0.78 ± 0.58	SPR	This study
Cladosporium fulvum	Avr4	CBM14	$(GlcNAc)_6$	6.3 ± 0.23	ITC	(Van Den Burg et al. 2004)
Cladosporium fulvum	Ecp6	CBM50	$(GlcNAc)_{4,5,6,8}$	11.5 to 3.7	ITC	(de Jonge et al. 2010)
PLANT						
Arabidopsis thaliana	AtLYK5	CBM50	$(GlcNAc)_8$	1.72	ITC	(Cao et al. 2014)
Hevea brasiliensis	Hevein	CBM18	$(GlcNAc)_5$	2.1	ITC	(Asensio et al. 2000)
Arabidopsis thaliana	AtCERK1	CBM50	$(GlcNAc)_8$	455	ITC	(Cao et al. 2014)
Arabidopsis thaliana	AtCERK1	CBM50	$(GlcNAc)_8$	448	ITC	(Liu et al. 2012)

ITC, isothermal titration calorimetry; SPR, surface plasmon resonance, CBM, carbohydrate-binding module; GlcNAc, N-Acetylglucosamin; Bio, biotinylated; [a] Ecp6 displays biphasic binding of chitin hexamer in pM range to LysM1-LysM3 groove and in µM range to LysM2 domain.

Table 2. The results of homology modelling of the VnaChtBP using the SWISS-MODEL server.

	Template	Description	Seq Identity	Oligo-States	GMOE	QMEAN	Coverage
Model01	2uwg.1.A	Wheat germ lectin	43.98%	Homo-dimer	0.31	-4.61	98-318
Model02	2wgc.1.A	Agglutin isolectin 1	40.96%	Homo-dimer	0.32	-3.22	39-254
Model03	1ulk.1.A	Lectin-C	49.15%	Homo-dimer	0.20	-0.65	212-378

Figure captions

Fig. 1. Domain architecture (A-D) and gene expression (E) of CBM18-containing proteins identified in *Verticillium nonalfalfae*. Protein organization was determined by querying protein sequences against CATH-Gene3D (Dawson et al. 2017) using the FunFHMMer web server and presented by IBS software (Liu et al. 2015). Proteins were classified into four groups: Lectin-like proteins (A), Chitinases (B), Chitin deacetlyases (C) and Xyloglucan endotransglucosylase (D). Gene expression is presented as a heatmap of log_2CPM values determined by RNA sequencing of infected hop (Progar et al. 2017).

Fig. 2. *VnaChtBP*, a gene encoding the CBM18 chitin binding protein of *Verticillium nonalfalfae*, is highly expressed in stems of susceptible hop at the late stages of infection. The gene expression of *VnaChtBP* was quantified by RT-qPCR using cDNA prepared from the roots and shoots of infected susceptible ('Celeia') and resistant ('Wye Target') hop plants (n = 5) at 6, 12 and 18 dpi and the expression levels were normalised relative to the expression of the gene in ½ liquid Czapek-Dox medium using topoisomerase (*VnaUn.148*) and splicing factor 3a2 (*Vna8.801*) as housekeeping genes (Marton et al. 2018). One way ANOVA with Tukey's post hoc test was performed to test for differences between the group means. FC, fold change; dpi, days post inoculation.

Fig. 3. A carbohydrate sedimentation test confirmed that the recombinant protein VnaChtBP specifically binds to chitin. A recombinant protein (15 µg) that bound to chitin beads and crab shell chitin was detected in the sediment, and it was present in the supernatant when incubated with cellulose, xylan or without the addition of carbohydrates (control). Western blot analysis was performed with primary antibody His-probe (H-3) (SCBT) (1:1,000) and secondary chicken anti-mouse IgG-HRP (SCBT) (1:5,000). Protein bands were detected using Super Signal West Pico (ThermoFisher Scientific) ECL substrate in a GelDoc-It2 Imager (UVP).

Fig. 4. SPR analysis of chitin hexamer binding to VnaChtBP. Different concentrations (0.05, 0.1, 0.2, 0.4, 0.8, 1.6, 3.2 and 6.4 µM) of $(GlcNAc)_6$ were tested for the binding (top panel). The binding curve (bottom panel) was generated by fitting steady state response levels at the end of the association phase, versus the concentration of the injected chitin hexamer. K_d was obtained by fitting the data to the steady-state affinity model. For reproducibility of binding, three independent titration experiments were performed. $(GlcNAc)_6$, hexa-N-acetyl chitohexaose

Fig 5. VnaChtBP protects fungus against degradation by plant chitinases. Micrographs of *Trichoderma viride* germinating spores, preincubated at RT for 2 h with 3 µM VnaChtBP, followed by the addition of xylem sap (19 U of chitinase/mg total protein) from *V. nonalfalfae* infected hop, were taken 24 h after treatment. The recombinant protein VnaChtBP caused aggregation and compaction of *T. viride* hyphae and protected the fungus from degradation by xylem sap chitinases. The chitinase activity of xylem sap was measured as a release of dye from Chitin Azure and one chitinase unit was defined as the amount of enzyme that caused a 0.01 increase in absorbance at 575 nm, measured at pH 5.0 and 25°C.

Fig. 6. VnaChtBP prevents chitin-induced activation of plant immune receptors. Reactive oxygen species (ROS) released from hop suspension cells in response to chitin hexamer $(GlcNAc)_6$ were measured using a chemiluminescent assay with 100 µM luminol-based substrate L-012 and 40 µg/ml horseradish

peroxidase. Generation of ROS was elicited with 1 µM $(GlcNAc)_6$ in the absence and presence of 5 µM VnaChtBP or with 5 µM VnaChtBP for control. Data were background-corrected and presented as a median with 95% confidence interval of 5 measurements. The area under the curve of the chitin-treated group, VnaChtBP-treated group and the chitin plus VnaChtBP group were compared using a non-parametric Kruskal-Wallis test with Holm's post hoc analysis(p-value < $2.2e^{-16}$).

Fig. 7. Confirmation of VnaChtBP dimerization (A), CD spectra of VnaChtBP in the absence and presence of chitin hexamer (B) and a schematic representation of the VnaChtBP homology model in complex with chitin hexamer (C). A: The effector gene *VnaChtBP* was cloned into the vectors pDEST22 and pDEST32 to serve as both bait and prey and yeast-two-hybrid assay was performed. Weak dimerization of the effector was confirmed on a triple dropout reporter media SC-LWH and no self-activation of the pDEST22 construct with empty pDEST32 vector was detected on the X-gal reporter. B: CD spectra of 2.5 µM VnaChtBP in the absence and presence of 25 µM chitin hexamer ($(GlcNAc)_6$) were recorded on a Jasco J-1500 CD spectrometer at 25 °C and pH 8.0. Binding of chitin hexamer to VnaChtBP induced additional secondary structure formation. C: The 3D model of VnaChtBP obtained by Swiss-Model (Arnold et al. 2006; Waterhouse et al. 2018) was refined by YASARA Structure (Krieger and Vriend 2014, 2015) and used in YASARA's AutoDock VINA module (Trott and Olson 2010) for molecular docking of chitin hexamer, built in the SWEET PROGRAM (Bohne et al. 1998, 1999). VnaChtBP is in dimeric form, the chitin binding domains of the Chain A (Chain B) are in cyan (grey) color shades. The chitin hexamer is shown in stick representation.

Fig. 8. Symptom development (A) and disease severity index (DSI) assessment (B) in susceptible hop following infection with the wild type *V. nonalfalfae* and two knockout mutants of *VnaChtBP*. Plants of susceptible hop 'Celeia' were inoculated by root dipping in 5×10^6 conidia/ml suspension and Verticillium wilting symptoms were assessed five times post inoculation. A: Both *VnaChtBP* deletion mutants displayed Verticillium wilting symptoms (chlorosis and necrosis of the leaves) in susceptible hop similar to the wild type fungus. Pictures were taken 35 days post inoculation. B: According to the DSI assessment with a 0-5 scale (Radišek et al. 2003), there were no significant differences between the wild type *V. nonalfalfae* and knockout mutants of *VnaChtBP*. Means with SE were calculated for 10 plants per treatment. Dpi, days post inoculation.

Supplementary Information

e-Xtra Table S1 lists *Verticillium* spp. isolates examined for the presence of *VnaChtBP*.

e-Xtra Table S2 shows sequence conservation of the closest VnaChtBP homologs as determined by *blastp* analysis against the NCBI non-redundant database.

e-Xtra Table S3 lists primers used for cloning, gene disruption and expression of VnaChtBP, fungal identification and relative biomass quantification.

e-Xtra File S1 presents the results of *NCBI BLAST+* query with the VnaChtBP sequence against the UniProt Knowledgebase at Interpro, summarizing protein family and domain predictions of homologous proteins.

e-Xtra File S2 contains the *Clustal O* nucleotide sequence alignment of the *V. nonalfalfae VnaChtBP* gene, *V. alfalfae VaChtBP* gene and the corresponding translation to the amino acid sequence with marked non-synonymous substitutions.

e-Xtra Fig. S1 shows domain architecture and gene expression of likely LysM effector proteins identified in *Verticillium nonalfalfae*. Protein organization was determined by matching protein sequences against the InterPro protein signature databases using the InterProScan tool. Results were presented by IBS software (Liu et al. 2015). Gene expression is presented as a heatmap of $\log_2$CPM values determined by RNA sequencing of infected hop (Progar et al. 2017).

e-Xtra Fig. S2 presents SDS-PAGE and western blot analysis of recombinant VnaChtBP production. Protein was expressed overnight at 16°C in *E. coli* SHuffle T7 cells (A), refolded from inclusion bodies (IB) using a mild solubilization method (Qi et al. 2015) and Ni-NTA affinity purified (B). Protein samples were separated by SDS-PAGE, transferred to a PVDF membrane and stained with Ponceau S. Western blot analysis was performed with primary antibody His-probe (H-3) (SCBT) (1:1,000) and secondary Chicken anti-mouse IgG-HRP (SCBT) (1:5,000). Protein bands were detected in the UVP gel imaging system using ECL substrate. T, total proteins; S, supernatant; P, pellet

e-Xtra Fig. S3 shows binding of various carbohydrates to recombinant VnaChtBP. Protein (0.1 mg/ml) was immobilized to the surface of a CM5 sensor chip and binding of N-acetyl glucosamine (NAG), glucosamine (GlcN), glucose (Glc), galactose (Gal) and mannose (Man) at a 500 µM concentration in HBS buffer (10 mM HEPES, 140 mM NaCl, pH 7.4) was monitored on Biacore T100.

e-Xtra Fig. S4 presents the morphology, sporulation and infectivity of *Verticillium nonalfalfae* wild type and *VnaChtBP* knockout mutants (A) and relative fungal biomass quantification in infected hop (B). Sporulation assessment 5 denotes 100% conidiation, while 1 denotes 20% conidiation of the wild type. Infectivity of 100% means all plants were infected with *V. nonalfalfae* as determined by fungal re-isolation from infected hop. The relative quantity of *V. nonalfalfae* DNA in infected hop was estimated at 21 dpi with the $2^{-\Delta\Delta Ct}$ method (Schmittgen and Livak 2008) using *V. nonalfalfae* lethal genotype (PG2) specific primer 5-1gs (Radišek et al. 2004) and hop reference gene DRH1 (DEAD box RNA helicase) for normalization (Štajner et al. 2013). Amplification levels are expressed relative to those obtained from plants infected with the wild type strain. One-way ANOVA with Tukey's multiple comparison test was performed in GraphPad Prism 8.02 (GraphPad Software, San Diego, California USA, www.graphpad.com) to test for difference between the wild type and mutant group means.

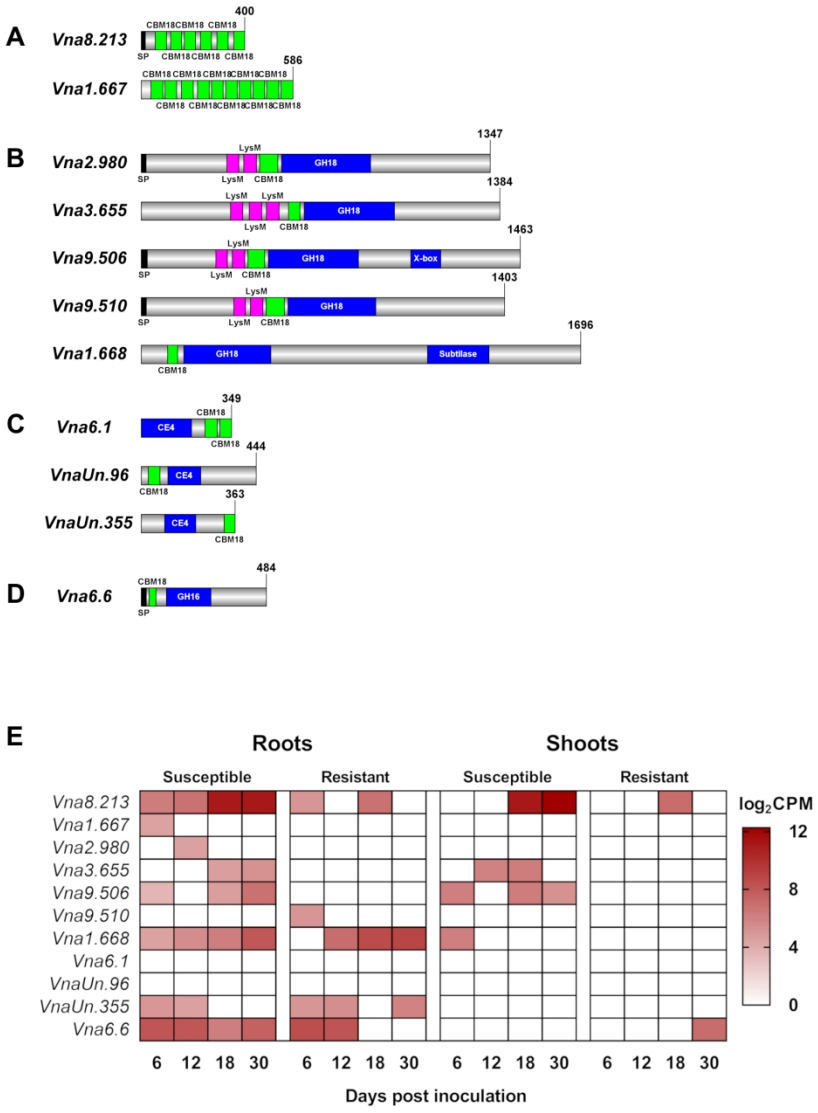

Domain architecture (A-D) and gene expression (E) of CBM18-containing proteins identified in *Verticillium nonalfalfae*. Protein organization was determined by querying protein sequences against CATH-Gene3D (Dawson et al. 2017) using the FunFHMMer web server and presented by IBS software (Liu et al. 2015). Proteins were classified into four groups: Lectin-like proteins (A), Chitinases (B), Chitin deacetlyases (C) and Xyloglucan endotransglucosylase (D). Gene expression is presented as a heatmap of log_2CPM values determined by RNA sequencing of infected hop (Progar et al. 2017).

177x246mm (300 x 300 DPI)

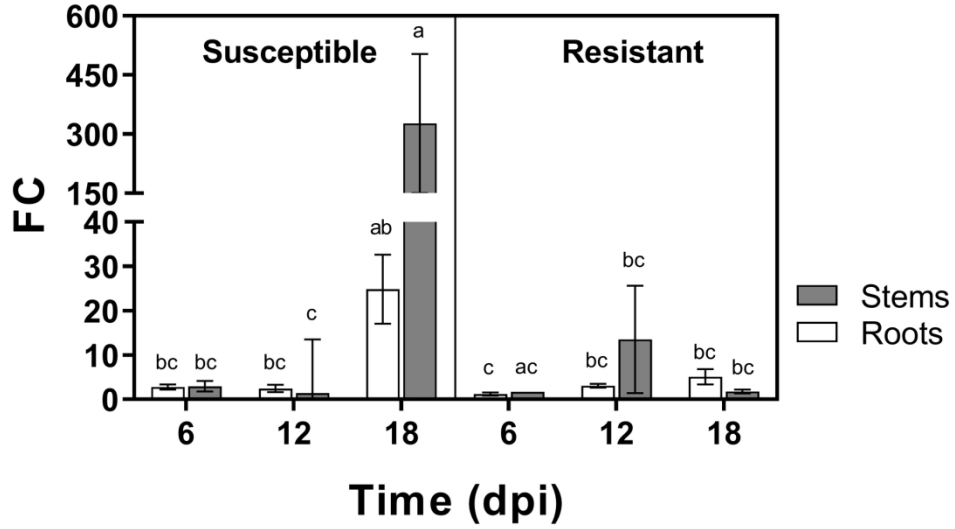

VnaChtBP, a gene encoding the CBM18 chitin binding protein of *Verticillium nonalfalfae*, is highly expressed in stems of susceptible hop at the late stages of infection. The gene expression of *VnaChtBP* was quantified by RT-qPCR using cDNA prepared from the roots and shoots of infected susceptible ('Celeia') and resistant ('Wye Target') hop plants (n = 5) at 6, 12 and 18 dpi and the expression levels were normalised relative to the expression of the gene in ½ liquid Czapek-Dox medium using topoisomerase (*VnaUn.148*) and splicing factor 3a2 (*Vna8.801*) as housekeeping genes (Marton et al. 2018). One way ANOVA with Tukey's post hoc test was performed to test for differences between the group means. FC, fold change; dpi, days post inoculation.

170x101mm (300 x 300 DPI)

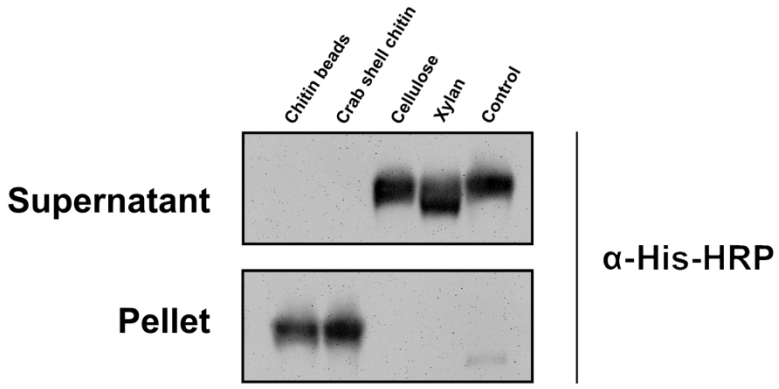

A carbohydrate sedimentation test confirmed that the recombinant protein VnaChtBP specifically binds to chitin. A recombinant protein (15 µg) that bound to chitin beads and crab shell chitin was detected in the sediment, and it was present in the supernatant when incubated with cellulose, xylan or without the addition of carbohydrates (control). Western blot analysis was performed with primary antibody His-probe (H-3) (SCBT) (1:1,000) and secondary chicken anti-mouse IgG-HRP (SCBT) (1:5,000). Protein bands were detected using Super Signal West Pico (ThermoFisher Scientific) ECL substrate in a GelDoc-It2 Imager (UVP).

215x101mm (300 x 300 DPI)

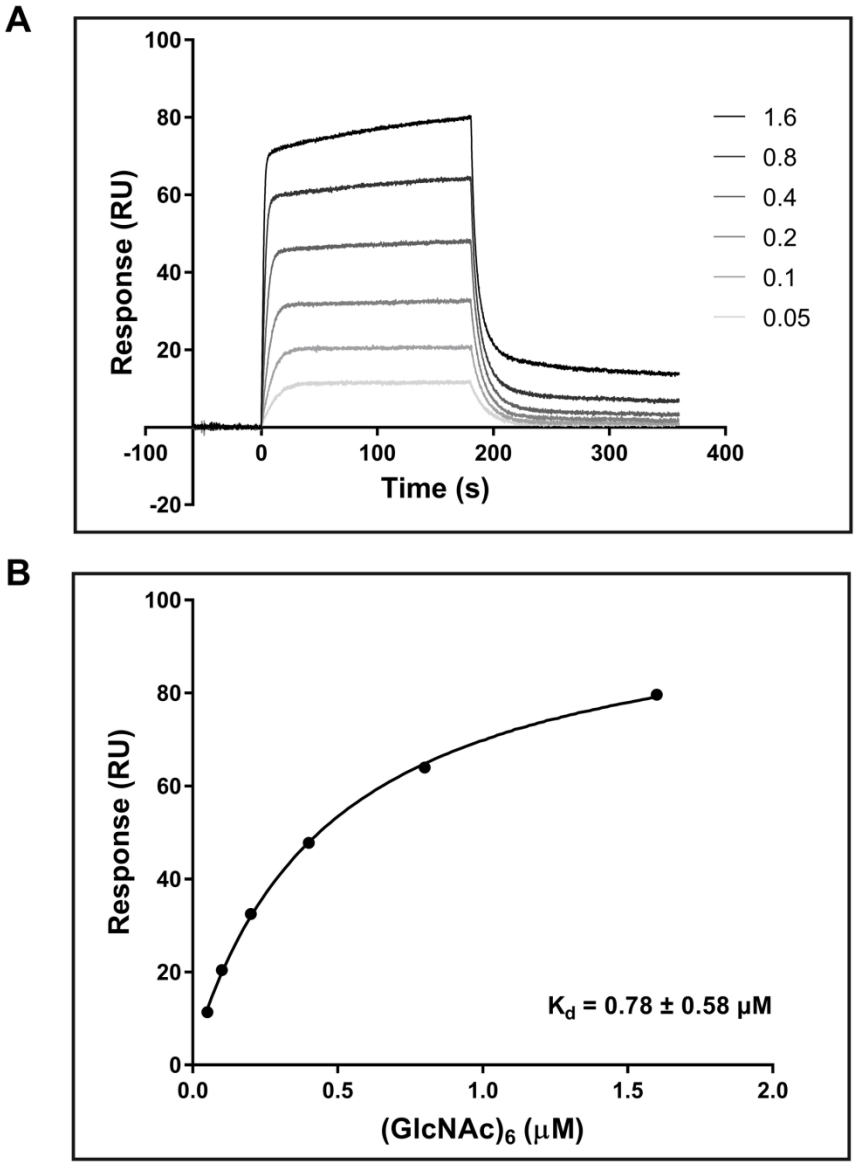

SPR analysis of chitin hexamer binding to VnaChtBP. Different concentrations (0.05, 0.1, 0.2, 0.4, 0.8, 1.6, 3.2 and 6.4 μM) of $(GlcNAc)_6$ were tested for the binding (top panel). The binding curve (bottom panel) was generated by fitting steady state response levels at the end of the association phase, versus the concentration of the injected chitin hexamer. K_d was obtained by fitting the data to the steady-state affinity model. For reproducibility of binding, three independent titration experiments were performed. $(GlcNAc)_6$, hexa-N-acetyl chitohexaose

177x244mm (300 x 300 DPI)

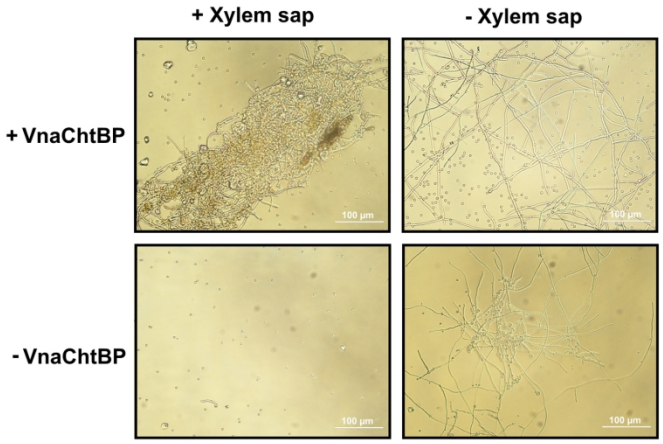

VnaChtBP protects fungus against degradation by plant chitinases. Micrographs of *Trichoderma viride* germinating spores, preincubated at RT for 2 h with 3 µM VnaChtBP, followed by the addition of xylem sap (19 U of chitinase/mg total protein) from *V. nonalfalfae* infected hop, were taken 24 h after treatment. The recombinant protein VnaChtBP caused aggregation and compaction of *T. viride* hyphae and protected the fungus from degradation by xylem sap chitinases. The chitinase activity of xylem sap was measured as a release of dye from Chitin Azure and one chitinase unit was defined as the amount of enzyme that caused a 0.01 increase in absorbance at 575 nm, measured at pH 5.0 and 25°C.

177x94mm (300 x 300 DPI)

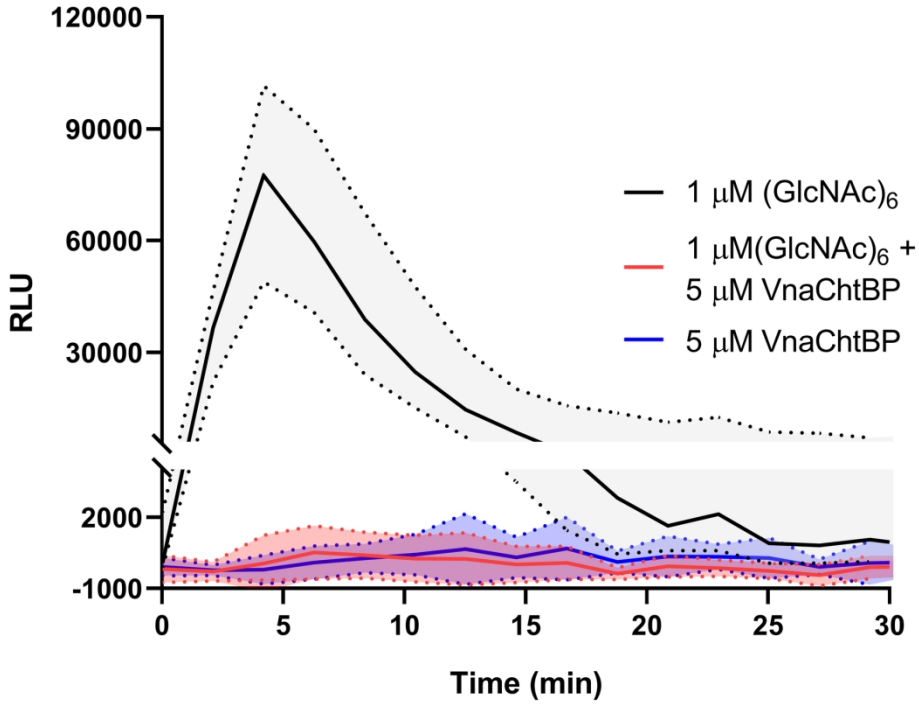

VnaChtBP prevents chitin-induced activation of plant immune receptors. Reactive oxygen species (ROS) released from hop suspension cells in response to chitin hexamer $(GlcNAc)_6$ were measured using a chemiluminescent assay with 100 µM luminol-based substrate L-012 and 40 µg/ml horseradish peroxidase. Generation of ROS was elicited with 1 µM $(GlcNAc)_6$ in the absence and presence of 5 µM VnaChtBP or with 5 µM VnaChtBP for control. Data were background-corrected and presented as a median with 95% confidence interval of 5 measurements. The area under the curve of the chitin-treated group, VnaChtBP-treated group and the chitin plus VnaChtBP group were compared using a non-parametric Kruskal-Wallis test with Holm's post hoc analysis($p\text{-value} < 2.2e^{-16}$).

170x129mm (300 x 300 DPI)

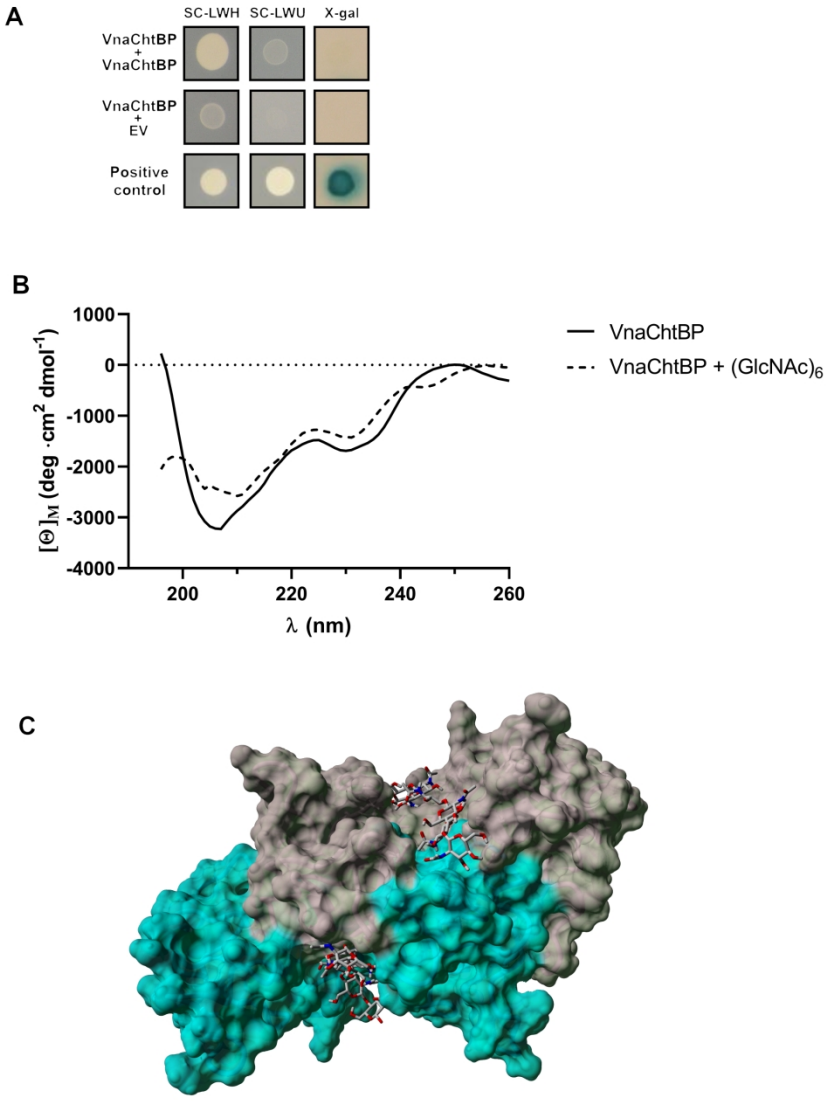

Confirmation of VnaChtBP dimerization (A), CD spectra of VnaChtBP in the absence and presence of chitin hexamer (B) and a schematic representation of the VnaChtBP homology model in complex with chitin hexamer (C). A: The effector gene VnaChtBP was cloned into the vectors pDEST22 and pDEST32 to serve as both bait and prey and yeast-two-hybrid assay was performed. Weak dimerization of the effector was confirmed on a triple dropout reporter media SC-LWH and no self-activation of the pDEST22 construct with empty pDEST32 vector was detected on the X-gal reporter. B: CD spectra of 2.5 μM VnaChtBP in the absence and presence of 25 μM chitin hexamer ((GlcNAc)6) were recorded on a Jasco J-1500 CD spectrometer at 25 °C and pH 8.0. Binding of chitin hexamer to VnaChtBP induced additional secondary structure formation. C: The 3D model of VnaChtBP obtained by Swiss-Model (Arnold et al. 2006; Waterhouse et al. 2018) was refined by YASARA Structure (Krieger and Vriend 2014, 2015) and used in YASARA's AutoDock VINA module (Trott and Olson 2010) for molecular docking of chitin hexamer, built in the SWEET PROGRAM (Bohne et al. 1998, 1999). VnaChtBP is in dimeric form, the chitin binding domains of the Chain A (Chain B) are in cyan (grey) color shades. The chitin hexamer is shown in stick representation.

177x245mm (300 x 300 DPI)

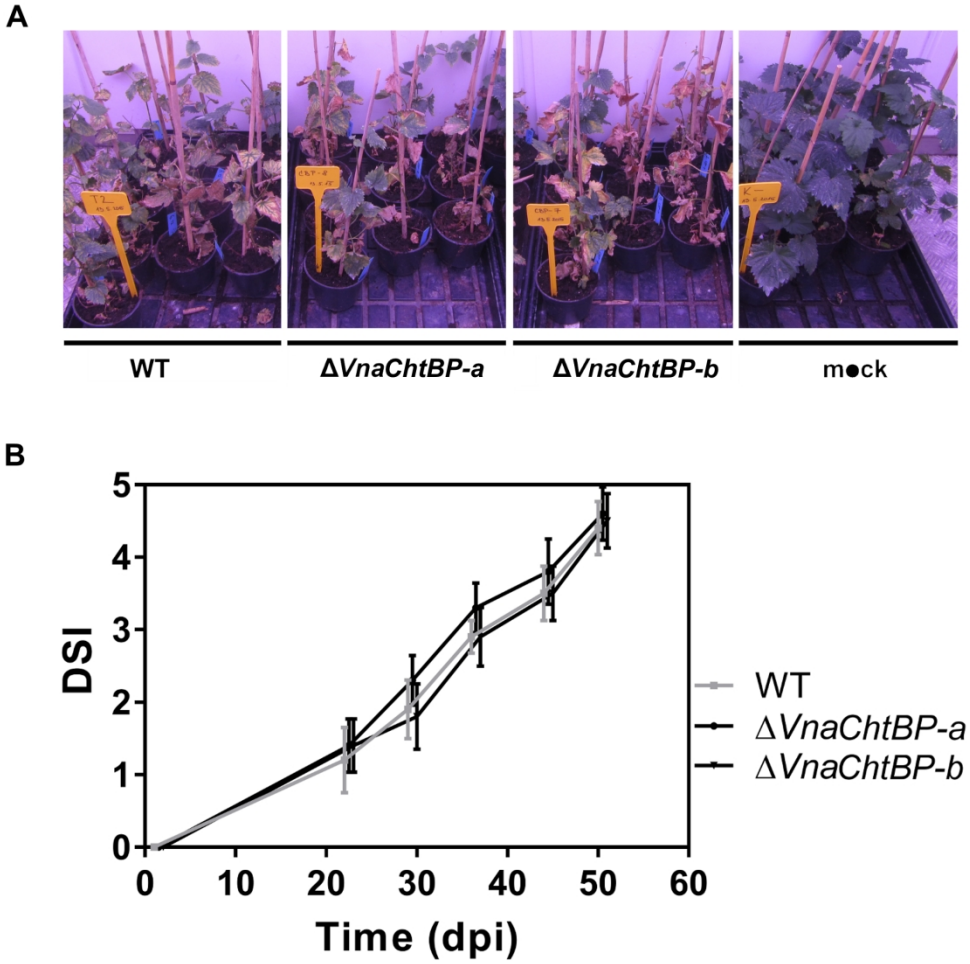

Symptom development (A) and disease severity index (DSI) assessment (B) in susceptible hop following infection with the wild type *V. nonalfalfae* and two knockout mutants of *VnaChtBP*. Plants of susceptible hop 'Celeia' were inoculated by root dipping in 5×10^6 conidia/ml suspension and Verticillium wilting symptoms were assessed five times post inoculation. A: Both *VnaChtBP* deletion mutants displayed Verticillium wilting symptoms (chlorosis and necrosis of the leaves) in susceptible hop similar to the wild type fungus. Pictures were taken 35 days post inoculation. B: According to the DSI assessment with a 0-5 scale (Radišek et al. 2003), there were no significant differences between the wild type *V. nonalfalfae* and knockout mutants of *VnaChtBP*. Means with SE were calculated for 10 plants per treatment. Dpi, days post inoculation.

blastp (version: BLASTP 2.7.1+)
Database: uniprotkb
Sequence: VNA8.2131-400
Length: 400

Sun, Jul 01, 2018 at 13:33:10
Sun, Jul 01, 2018 at 13:34:15

Fast Family and Domain Prediction
(Query Sequence View)

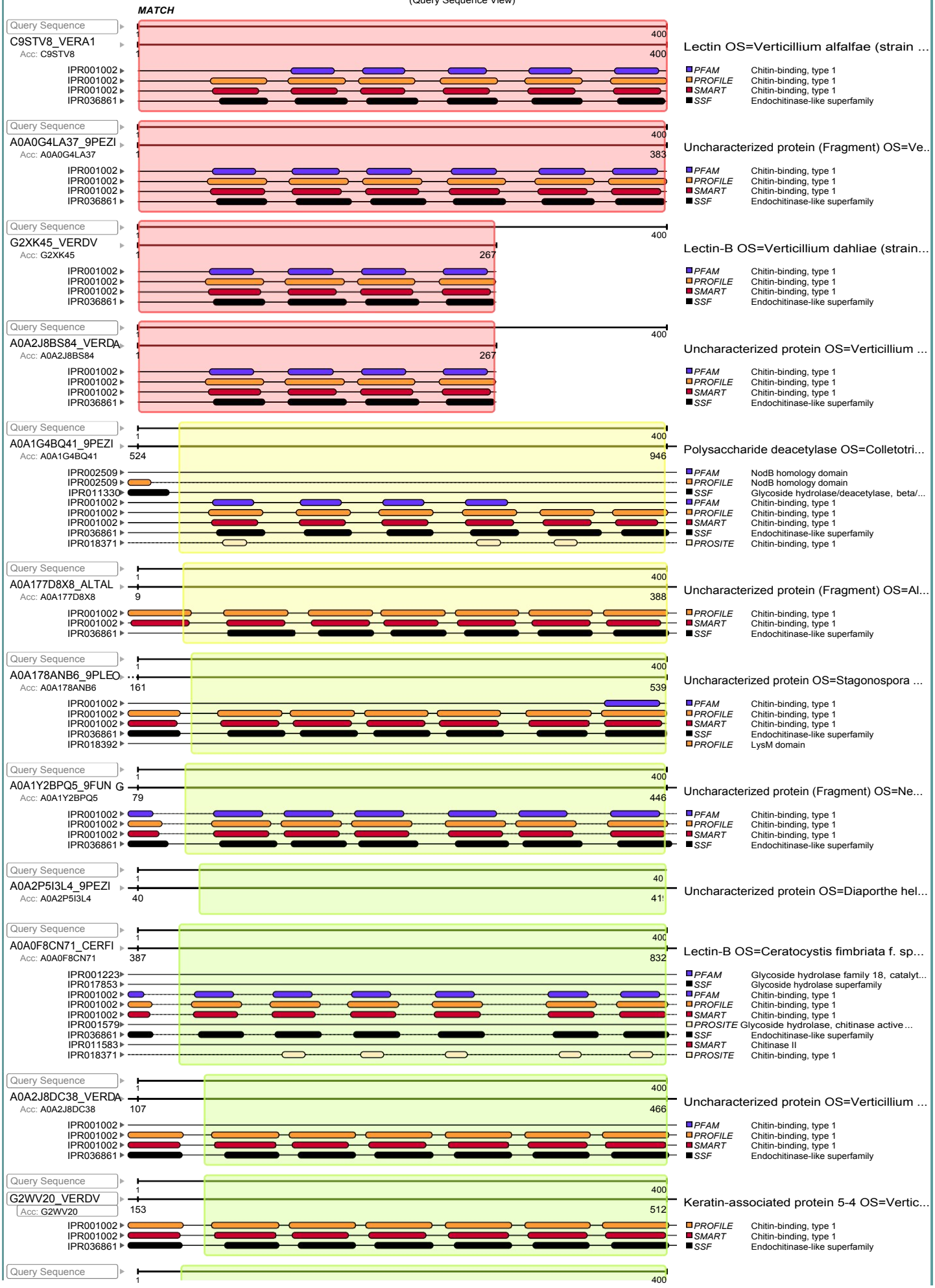

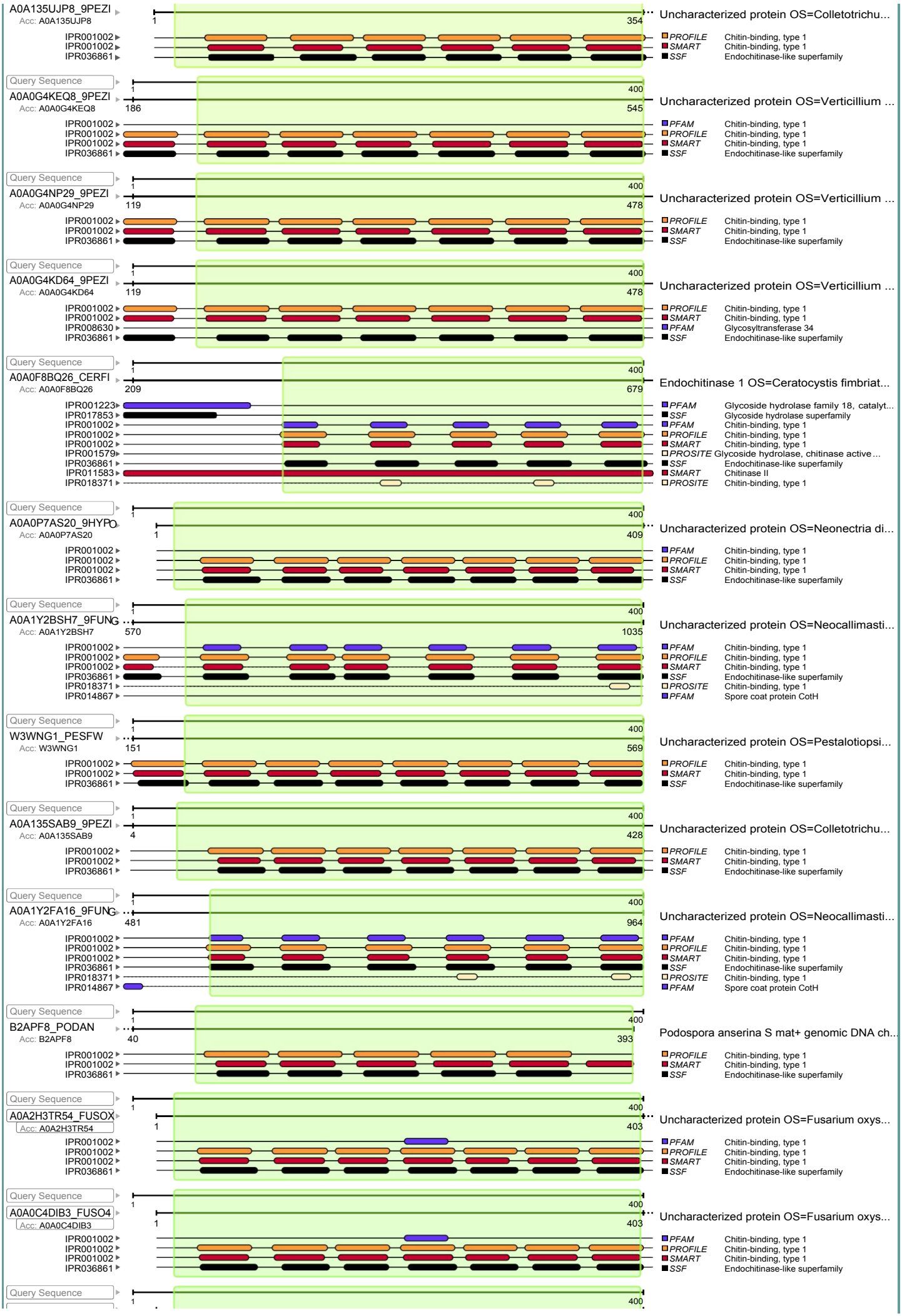
A0A135UJP8_9PEZI
Acc: A0A135UJP8
1
354
Uncharacterized protein OS=Colletotrichu...
IPR001002
IPR001002
IPR036861
PROFILE Chitin-binding, type 1
SMART Chitin-binding, type 1
SSF Endochitinase-like superfamily
Query Sequence
A0A0G4KEQ8_9PEZI
Acc: A0A0G4KEQ8
186
545
Uncharacterized protein OS=Verticillium ...
IPR001002
IPR001002
IPR001002
IPR036861
PFAM Chitin-binding, type 1
PROFILE Chitin-binding, type 1
SMART Chitin-binding, type 1
SSF Endochitinase-like superfamily
Query Sequence
A0A0G4NP29_9PEZI
Acc: A0A0G4NP29
119
478
Uncharacterized protein OS=Verticillium ...
IPR001002
IPR001002
IPR036861
PROFILE Chitin-binding, type 1
SMART Chitin-binding, type 1
SSF Endochitinase-like superfamily
Query Sequence
A0A0G4KD64_9PEZI
Acc: A0A0G4KD64
119
478
Uncharacterized protein OS=Verticillium ...
IPR001002
IPR001002
IPR008630
IPR036861
PROFILE Chitin-binding, type 1
SMART Chitin-binding, type 1
PFAM Glycosyltransferase 34
SSF Endochitinase-like superfamily
Query Sequence
A0A0F8BQ26_CERFI
Acc: A0A0F8BQ26
209
679
Endochitinase 1 OS=Ceratocystis fimbriat...
IPR001223
IPR017853
IPR001002
IPR001002
IPR001002
IPR001579
IPR036861
IPR011583
IPR018371
PFAM Glycoside hydrolase family 18, catalyt...
SSF Glycoside hydrolase superfamily
PFAM Chitin-binding, type 1
PROFILE Chitin-binding, type 1
SMART Chitin-binding, type 1
PROSITE Glycoside hydrolase, chitinase active ...
SSF Endochitinase-like superfamily
SMART Chitinase II
PROSITE Chitin-binding, type 1
Query Sequence
A0A0P7AS20_9HYPO
Acc: A0A0P7AS20
1
409
Uncharacterized protein OS=Neonectria di...
IPR001002
IPR001002
IPR001002
IPR036861
PFAM Chitin-binding, type 1
PROFILE Chitin-binding, type 1
SMART Chitin-binding, type 1
SSF Endochitinase-like superfamily
Query Sequence
A0A1Y2BSH7_9FUNG
Acc: A0A1Y2BSH7
570
1035
Uncharacterized protein OS=Neocallimasti...
IPR001002
IPR001002
IPR001002
IPR036861
IPR018371
IPR014867
PFAM Chitin-binding, type 1
PROFILE Chitin-binding, type 1
SMART Chitin-binding, type 1
SSF Endochitinase-like superfamily
PROSITE Chitin-binding, type 1
PFAM Spore coat protein CotH
Query Sequence
W3WNG1_PESFW
Acc: W3WNG1
151
569
Uncharacterized protein OS=Pestalotiopsi...
IPR001002
IPR001002
IPR036861
PROFILE Chitin-binding, type 1
SMART Chitin-binding, type 1
SSF Endochitinase-like superfamily
Query Sequence
A0A135SAB9_9PEZI
Acc: A0A135SAB9
4
428
Uncharacterized protein OS=Colletotrichu...
IPR001002
IPR001002
IPR036861
PROFILE Chitin-binding, type 1
SMART Chitin-binding, type 1
SSF Endochitinase-like superfamily
Query Sequence
A0A1Y2FA16_9FUNG
Acc: A0A1Y2FA16
481
964
Uncharacterized protein OS=Neocallimasti...
IPR001002
IPR001002
IPR001002
IPR036861
IPR018371
IPR014867
PFAM Chitin-binding, type 1
PROFILE Chitin-binding, type 1
SMART Chitin-binding, type 1
SSF Endochitinase-like superfamily
PROSITE Chitin-binding, type 1
PFAM Spore coat protein CotH
Query Sequence
B2APF8_PODAN
Acc: B2APF8
40
393
Podospora anserina S mat+ genomic DNA ch...
IPR001002
IPR001002
IPR036861
PROFILE Chitin-binding, type 1
SMART Chitin-binding, type 1
SSF Endochitinase-like superfamily
Query Sequence
A0A2H3TR54_FUSOX
Acc: A0A2H3TR54
1
403
Uncharacterized protein OS=Fusarium oxys...
IPR001002
IPR001002
IPR001002
IPR036861
PFAM Chitin-binding, type 1
PROFILE Chitin-binding, type 1
SMART Chitin-binding, type 1
SSF Endochitinase-like superfamily
Query Sequence
A0A0C4DIB3_FUSO4
Acc: A0A0C4DIB3
1
403
Uncharacterized protein OS=Fusarium oxys...
IPR001002
IPR001002
IPR001002
IPR036861
PFAM Chitin-binding, type 1
PROFILE Chitin-binding, type 1
SMART Chitin-binding, type 1
SSF Endochitinase-like superfamily
Query Sequence

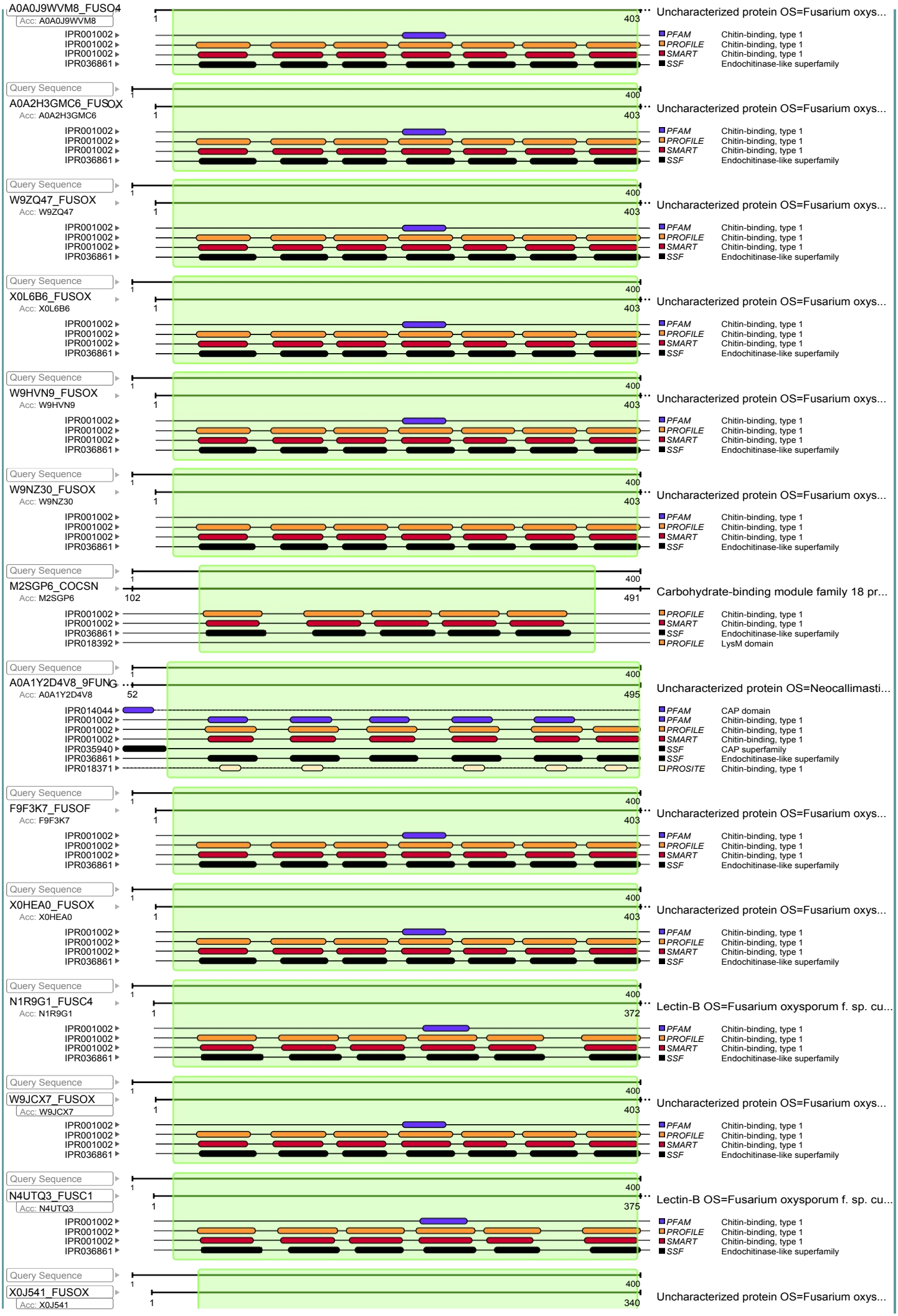
A0A0J9WVM8_FUSO4
Acc: A0A0J9WVM8
1
403
Uncharacterized protein OS=Fusarium oxys...
IPR001002
IPR001002
IPR001002
IPR036861
PFAM Chitin-binding, type 1
PROFILE Chitin-binding, type 1
SMART Chitin-binding, type 1
SSF Endochitinase-like superfamily
Query Sequence
1
400
A0A2H3GMC6_FUSOX
Acc: A0A2H3GMC6
1
403
Uncharacterized protein OS=Fusarium oxys...
IPR001002
IPR001002
IPR001002
IPR036861
PFAM Chitin-binding, type 1
PROFILE Chitin-binding, type 1
SMART Chitin-binding, type 1
SSF Endochitinase-like superfamily
Query Sequence
1
400
W9ZQ47_FUSOX
Acc: W9ZQ47
1
403
Uncharacterized protein OS=Fusarium oxys...
IPR001002
IPR001002
IPR001002
IPR036861
PFAM Chitin-binding, type 1
PROFILE Chitin-binding, type 1
SMART Chitin-binding, type 1
SSF Endochitinase-like superfamily
Query Sequence
1
400
X0L6B6_FUSOX
Acc: X0L6B6
1
403
Uncharacterized protein OS=Fusarium oxys...
IPR001002
IPR001002
IPR001002
IPR036861
PFAM Chitin-binding, type 1
PROFILE Chitin-binding, type 1
SMART Chitin-binding, type 1
SSF Endochitinase-like superfamily
Query Sequence
1
400
W9HVN9_FUSOX
Acc: W9HVN9
1
403
Uncharacterized protein OS=Fusarium oxys...
IPR001002
IPR001002
IPR001002
IPR036861
PFAM Chitin-binding, type 1
PROFILE Chitin-binding, type 1
SMART Chitin-binding, type 1
SSF Endochitinase-like superfamily
Query Sequence
1
400
W9NZ30_FUSOX
Acc: W9NZ30
1
403
Uncharacterized protein OS=Fusarium oxys...
IPR001002
IPR001002
IPR001002
IPR036861
PFAM Chitin-binding, type 1
PROFILE Chitin-binding, type 1
SMART Chitin-binding, type 1
SSF Endochitinase-like superfamily
Query Sequence
1
400
M2SGP6_COCSN
Acc: M2SGP6
102
491
Carbohydrate-binding module family 18 pr...
IPR001002
IPR001002
IPR036861
IPR018392
PROFILE Chitin-binding, type 1
SMART Chitin-binding, type 1
SSF Endochitinase-like superfamily
PROFILE LysM domain
Query Sequence
1
400
A0A1Y2D4V8_9FUNG
Acc: A0A1Y2D4V8
52
495
Uncharacterized protein OS=Neocallimasti...
IPR014044
IPR001002
IPR001002
IPR001002
IPR035940
IPR036861
IPR018371
PFAM CAP domain
PFAM Chitin-binding, type 1
PROFILE Chitin-binding, type 1
SMART Chitin-binding, type 1
SSF CAP superfamily
SSF Endochitinase-like superfamily
PROSITE Chitin-binding, type 1
Query Sequence
1
400
F9F3K7_FUSOF
Acc: F9F3K7
1
403
Uncharacterized protein OS=Fusarium oxys...
IPR001002
IPR001002
IPR001002
IPR036861
PFAM Chitin-binding, type 1
PROFILE Chitin-binding, type 1
SMART Chitin-binding, type 1
SSF Endochitinase-like superfamily
Query Sequence
1
400
X0HEA0_FUSOX
Acc: X0HEA0
1
403
Uncharacterized protein OS=Fusarium oxys...
IPR001002
IPR001002
IPR001002
IPR036861
PFAM Chitin-binding, type 1
PROFILE Chitin-binding, type 1
SMART Chitin-binding, type 1
SSF Endochitinase-like superfamily
Query Sequence
1
400
N1R9G1_FUSC4
Acc: N1R9G1
1
372
Lectin-B OS=Fusarium oxysporum f. sp. cu...
IPR001002
IPR001002
IPR001002
IPR036861
PFAM Chitin-binding, type 1
PROFILE Chitin-binding, type 1
SMART Chitin-binding, type 1
SSF Endochitinase-like superfamily
Query Sequence
1
400
W9JCX7_FUSOX
Acc: W9JCX7
1
403
Uncharacterized protein OS=Fusarium oxys...
IPR001002
IPR001002
IPR001002
IPR036861
PFAM Chitin-binding, type 1
PROFILE Chitin-binding, type 1
SMART Chitin-binding, type 1
SSF Endochitinase-like superfamily
Query Sequence
1
400
N4UTQ3_FUSC1
Acc: N4UTQ3
1
375
Lectin-B OS=Fusarium oxysporum f. sp. cu...
IPR001002
IPR001002
IPR001002
IPR036861
PFAM Chitin-binding, type 1
PROFILE Chitin-binding, type 1
SMART Chitin-binding, type 1
SSF Endochitinase-like superfamily
Query Sequence
1
400
X0J541_FUSOX
Acc: X0J541
1
340
Uncharacterized protein OS=Fusarium oxys...

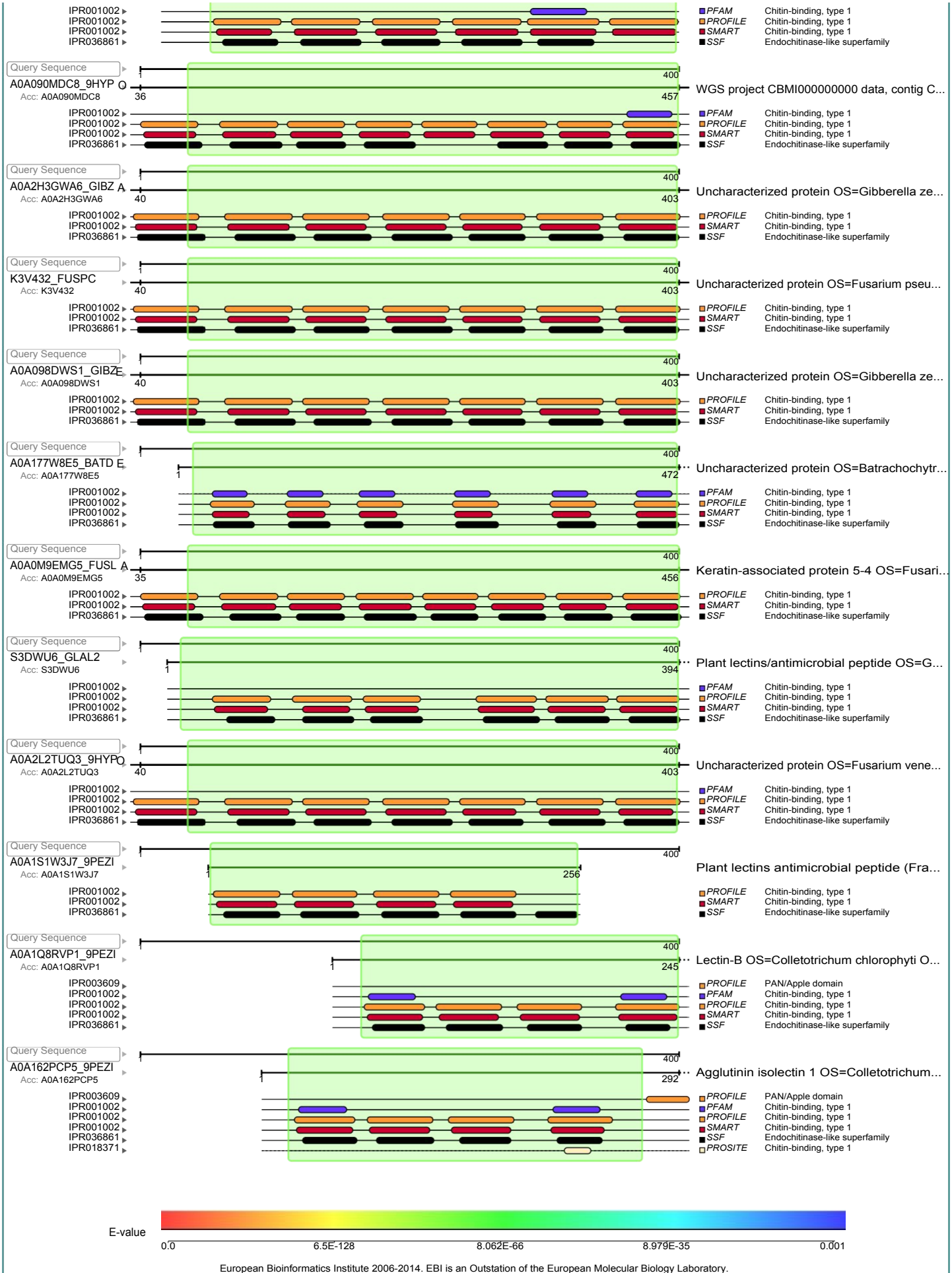

CLUSTAL O(1.2.4) multiple sequence alignment

Vna: DNA sequence of *VnaChtBP* (MH325205)
Va: DNA sequence of *VaCBP* (MH325206)
P_Vna: protein sequence of Vna*ChtBP*
Δ: amino-acid in the Va sequence that differs from Vna sequence
Underlined: SingalP
Grey: Chitin binding domain (ChtBD1; PF00187)
Boxed: Amino-acid change and the responsible SNP in the Vna-Va sequence alignment

```
Vna      ATGCGTTTCTCCGCCGTTCTTACCGCTCTGCTCGTGGCCTGCGCCGCGGCCAAACCTCAT   60
Va       ATGCGTTTCTCCGCCGTTCTTACCGCTCTGCTCGTGGCCTGTGCCGCGGCCAAACCTCAT   60
         ************************************* ******************

P_Vna    MetArgPheSerAlaValLeuThrAlaLeuLeuValAlaCysAlaAlaAlaLysProHis   20
Δ                                                                       20

Vna      GGCAAGCGTGACGTGTGCCCGGCCAAGCCCCCCAAGAGCAGCCAGTCGAGTACTGCAACA   120
Va       GGCAAGCGTGACGTGTGCCCGGCCAAGCCCCCCAAGAGCAGTCAGTCGAGCACTGCCACA   120
         ************************************* ******** ***** ***

P_Vna    GlyLysArgAspValCysProAlaLysProProLysSerSerGlnSerSerThrAlaThr   40
Δ                                                                       40


Vna      ACTACTAGCAGTAGGCCAGCCCCGACTGGGCCCTTTTCCGACGACGCCTCTTGCGGTGGC   180
Va       ACTACTAGCAGTAGGCCAGCCCCGACTGGCCCCTTTTCCGACGACGCCTCTTGCGGTGGA   180
         ***************************** *****************************

P_Vna    ThrThrSerSerArgProAlaProThrGlyProPheSerAspAspAlaSerCysGlyGly   60
Δ                                                                       60


Vna      CCCAACAACTTTGTCTGCCGCTCTGGGACATGCTGCTCCAGTGCCAACTTCTGCGGCGTC   240
Va       CCCAACAAATTCGTCTGCCGCTCTGGGACATGCTGCTCTAGTGCCAACTTCTGCGGCGTC   240
         ******** ** ************************* ********************

P_Vna    ProAsnAsnPheValCysArgSerGlyThrCysCysSerSerAlaAsnPheCysGlyVal   80
Δ              Arg                                                      80


Vna      ACTGCTGCCCACTGCGAGGCAGGCTGCCAACCTGGATTGGGTGATTGCGGCTCTCAATTC   300
Va       ACTGCTGCCCACTGCGAGGGAGGCTGCCGACCTGAATTGGGTGATTGCGGCTCTCAATTC   300
         ****************** ******** ***** ************************

P_Vna    ThrAlaAlaHisCysGluAlaGlyCysGlnProGlyLeuGlyAspCysGlySerGlnPhe   100
Δ                          Thr       Arg   Glu                         100


Vna      GTCAAAATCTCGACCGGGCCTCCTGGCAGTGTTTCGACCGACGGTACCTGCGGCGGCACC   360
Va       GTCAAAATCTCGACCGGGCCTCCTGGCAGTGTTTCGACCGACGGTACCTGCGGCGGCACC   360
         ************************************************************

P_Vna    ValLysIleSerThrGlyProProGlySerValSerThrAspGlyThrCysGlyGlyThr   120
Δ                                                                       120


Vna      AACGGCTGGATATGCCCCAAAGGCAACTGCTGCTCGCGATTCGGCTTCTGTGGTGCTACA   420
Va       AACGGCTGGATATGCCCCAAAGGCAACTGCTGCTCGCGATTCGGCTTCTGTGGTGCTACA   420
         ************************************************************

P_Vna    AsnGlyTrpIleCysProLysGlyAsnCysCysSerArgPheGlyPheCysGlyAlaThr   140
Δ                                                                       140


Vna      GCTGATCACTGCGCCCCCGGCTGCCAGCCCGCCTTTGGTATCTGTCCCAACCCCACCCCT   480
Va       GCTGATCACTGCGCCCCCGGCTGCCAGCCCACCTTTGGTATCTGTCCCAACCCCACCCCT   480
         ***************************** *****************************
```

```
P_Vna    AlaAspHisCysAlaProGlyCysGlnProAlaPheGlyIleCysProAsnProThrPro      160
Δ                                     Thr                                  160

Vna      GGCGGTAATGCCTCGCCTGACGGCACTTGCGGTGGCTCTAACAAGTTTATCTGCGCTTCC      540
Va       GGCGGTAATGCCTCGCCTGACGGCACTTGCGGTGGCTCTAACAAGTTTATCTGCGCTTCC      540
         ************************************************************

P_Vna    GlyGlyAsnAlaSerProAspGlyThrCysGlyGlySerAsnLysPheIleCysAlaSer      180
Δ                                                                          180

Vna      GGGACCTGCTGCTCCAAGGCTGGCTTCTGTGGTAACACTAAGGACCACTGCGACGCCGGC      600
Va       GGGACCTGCTGCTCTAAGGCTGGCTTCTGTGGTACTACTAAGGACCACTGCGACGCCGGC      600
         ************** ******************  ************************

P_Vna    GlyThrCysCysSerLysAlaGlyPheCysGlyAsnThrLysAspHisCysAspAlaGly      200
Δ                                     Thr                                  200

Vna      TGCCAGTTTGATTTTGGTAGCTGCGGCGACGCTTTCGTCCCGGTCCCGGGCGGTAATCCC      660
Va       TGCCAGTTTGATTTTGGTAGCTGCGGCGACGCTTTCGTCCCGGTCCCGGGCGGTAATCCC      660
         ************************************************************

P_Vna    CysGlnPheAspPheGlySerCysGlyAspAlaPheValProValProGlyGlyAsnPro      220
Δ                                                                          220

Vna      CCGCCCCGCGGTAGTGTCTCTACCGATGGCACCTGCGCTGGTGCTAACGGCTTGATCTGT      720
Va       CCGCCCCGCGGTAGTGTCTCTACCGATGGCACCTGCGCTGGTGCTAACGGCTTGATCTGT      720
         ************************************************************

P_Vna    ProProArgGlySerValSerThrAspGlyThrCysAlaGlyAlaAsnGlyLeuIleCys      240
Δ                                                                          240

Vna      CCTCAAGGCAACTGCTGCTCGCGATTTGGCTTCTGTGGTGCTACAGCTGATCACTGCGGC      780
Va       CCTCAAGGCAACTGCTGCTCGCGATTTGGCTTCTGTGGTGCTACGGCTGATCACTGCGGC      780
         ******************************************** ***************

P_Vna    ProGlnGlyAsnCysCysSerArgPheGlyPheCysGlyAlaThrAlaAspHisCysGly      260
Δ                                                                          260

Vna      ACCGGCTGTCAGTCAGCCTTCGGTATCTGTAACACCGGCGGTGCCACATCTTCTTCGACC      840
Va       ACCGACTGTCAGCCAGCCTTCGGTATCTGTAACACCGGCGGTGCTACATCTTCTTCGACC      840
         **** ******* ******************************** ***************

P_Vna    ThrGlyCysGlnSerAlaPheGlyIleCysAsnThrGlyGlyAlaThrSerSerSerThr      280
Δ           Asp      Pro                                                   280

Vna      AGCTCGAAGCCGGCCCCTACCGGCGGCATCTCGCCCGATGGCTCTTGCGGCGGCACCAAC      900
Va       AGCTCGAAGCCGGCCCCTACCGGCGGCATTTCGCCCGATGGCTCTTGCGGCGGCACCAAC      900
         ***************************** ******************************

P_Vna    SerSerLysProAlaProThrGlyGlyIleSerProAspGlySerCysGlyGlyThrAsn      300
Δ                                                                          300

Vna      GGCTTCACCTGCACACCGGGTAACTGCTGCTCACAGTTCGGCTTCTGTGGTGCTACGACT      960
Va       GGTTATACCTGCACACCGGGTAACTGCTGCTCACAGTTCGGGTTCTGCGGTGCTACGACT      960
         ** *  ********************************** ***** ************

P_Vna    GlyPheThrCysThrProGlyAsnCysCysSerGlnPheGlyPheCysGlyAlaThrThr      320
Δ           Tyr                                                            320

Vna      GGCCACTGCGGCACTGGTTGCCAGTCCGCCTTCGGTATCTGTGGCACCGGAGGCCCTGCG     1020
Va       GGCCACTGCGGCACTGGTTGTCAGTCAGCCTTCGGTATCTGTGGCACCGGCGGTGCTACC     1020
```

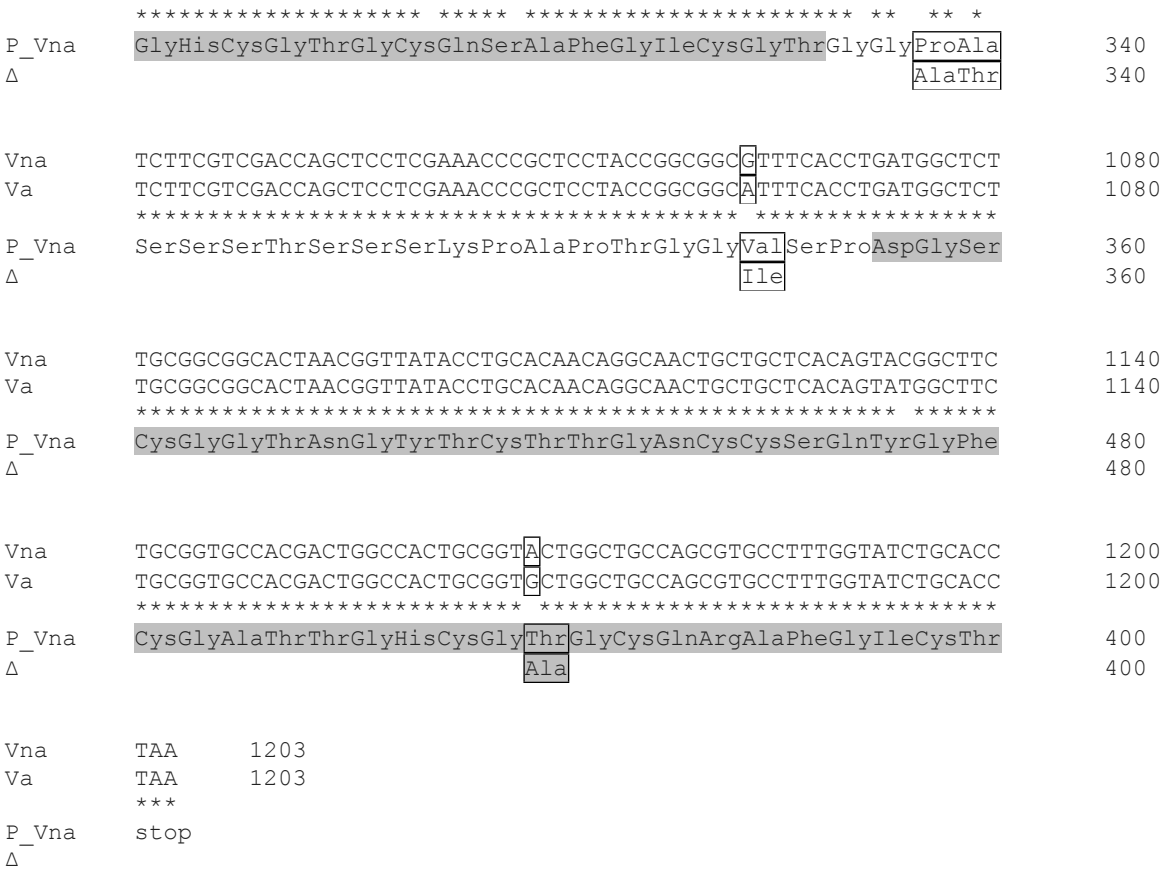
P_Vna GlyHisCysGlyThrGlyCysGlnSerAlaPheGlyIleCysGlyThrGlyGlyProAla 340
Δ AlaThr 340
Vna TCTTCGTCGACCAGCTCCTCGAAACCCGCTCCTACCGGCGGCGTTTCACCTGATGGCTCT 1080
Va TCTTCGTCGACCAGCTCCTCGAAACCCGCTCCTACCGGCGGCATTTCACCTGATGGCTCT 1080
P_Vna SerSerSerThrSerSerSerLysProAlaProThrGlyGlyValSerProAspGlySer 360
Δ Ile 360
Vna TGCGGCGGCACTAACGGTTATACCTGCACAACAGGCAACTGCTGCTCACAGTACGGCTTC 1140
Va TGCGGCGGCACTAACGGTTATACCTGCACAACAGGCAACTGCTGCTCACAGTATGGCTTC 1140
P_Vna CysGlyGlyThrAsnGlyTyrThrCysThrThrGlyAsnCysCysSerGlnTyrGlyPhe 480
Δ 480
Vna TGCGGTGCCACGACTGGCCACTGCGGTACTGGCTGCCAGCGTGCCTTTGGTATCTGCACC 1200
Va TGCGGTGCCACGACTGGCCACTGCGGTGCTGGCTGCCAGCGTGCCTTTGGTATCTGCACC 1200
P_Vna CysGlyAlaThrThrGlyHisCysGlyThrGlyCysGlnArgAlaPheGlyIleCysThr 400
Δ Ala 400
Vna TAA 1203
Va TAA 1203
P_Vna stop
Δ

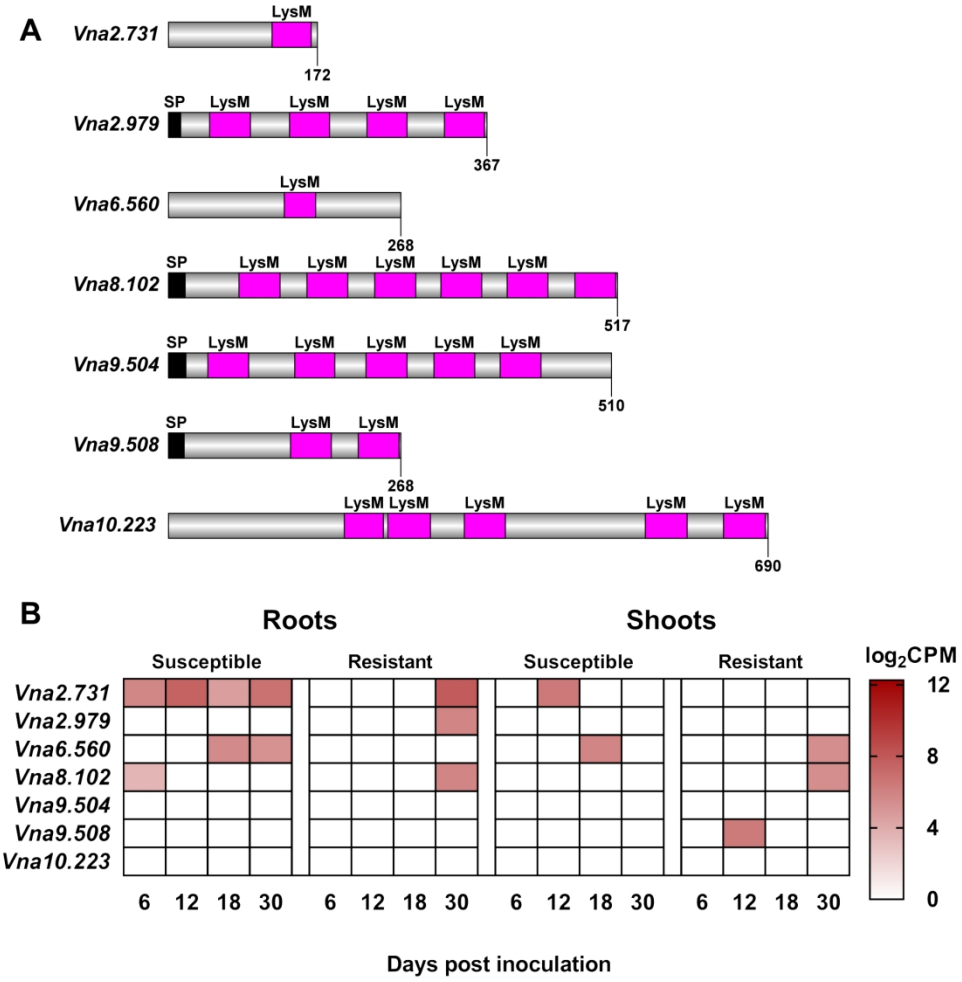

Domain architecture and gene expression of likely LysM effector proteins identified in *Verticillium nonalfalfae*. Protein organization was determined by matching protein sequences against the InterPro protein signature databases using the InterProScan tool. Results were presented by IBS software (Liu et al. 2015). Gene expression is presented as a heatmap of log_2CPM values determined by RNA sequencing of infected hop (Progar et al. 2017).

177x195mm (300 x 300 DPI)

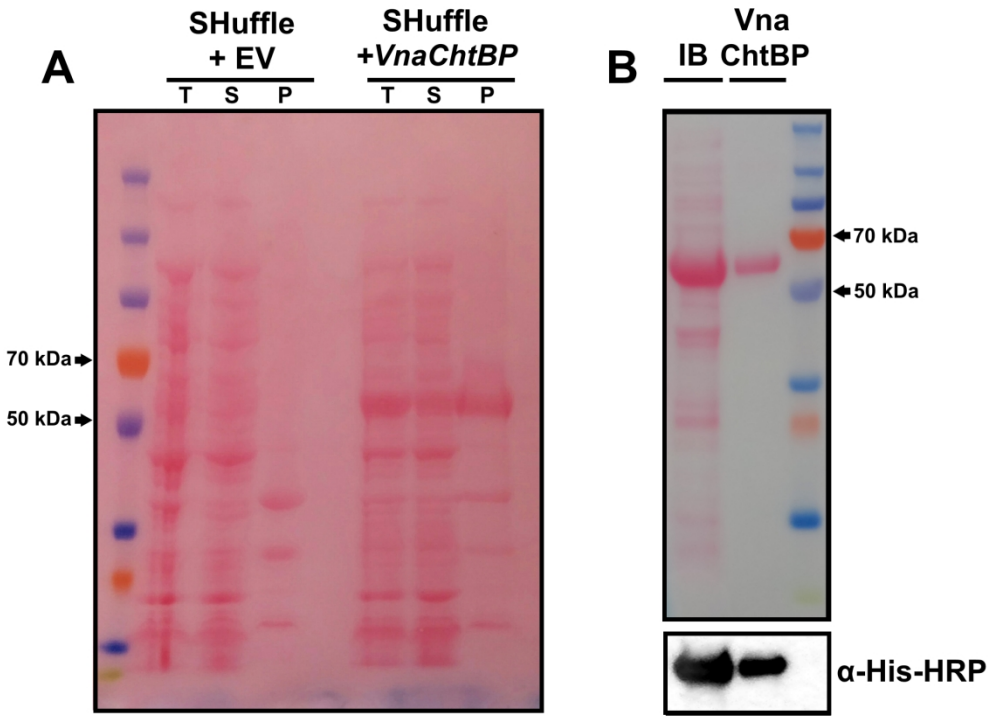

SDS-PAGE and western blot analysis of recombinant VnaChtBP production. Protein was expressed overnight at 16°C in *E. coli* SHuffle T7 cells (A), refolded from inclusion bodies (IB) using a mild solubilization method (Qi et al. 2015) and Ni-NTA affinity purified (B). Protein samples were separated by SDS-PAGE, transferred to a PVDF membrane and stained with Ponceau S. Western blot analysis was performed with primary antibody His-probe (H-3) (SCBT) (1:1,000) and secondary Chicken anti-mouse IgG-HRP (SCBT) (1:5,000). Protein bands were detected in the UVP gel imaging system using ECL substrate. T, total proteins; S, supernatant; P, pellet

177x169mm (300 x 300 DPI)

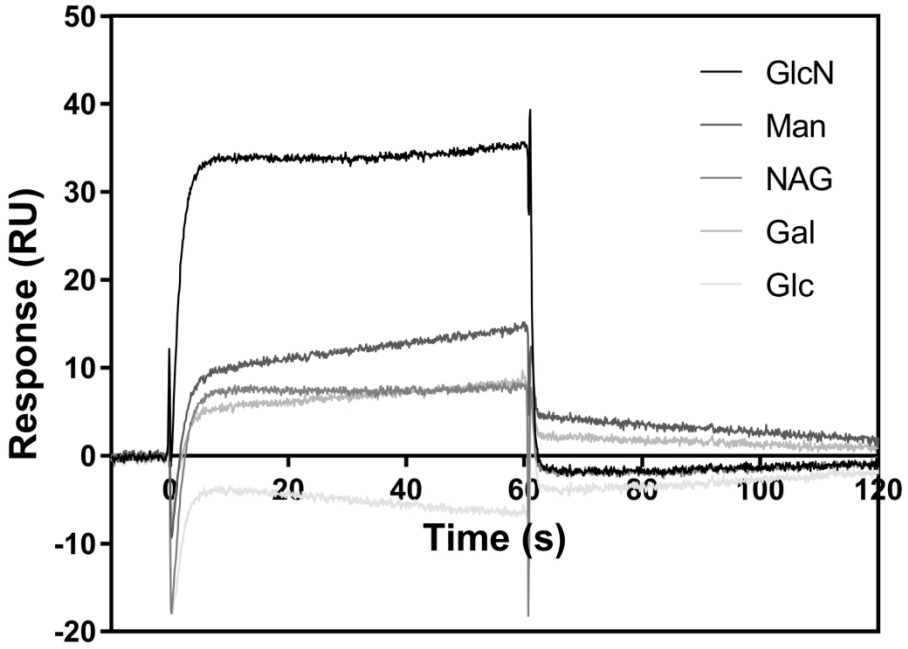

Binding of various carbohydrates to recombinant VnaChtBP. Protein (0.1 mg/ml) was immobilized to the surface of a CM5 sensor chip and binding of N-acetyl glucosamine (NAG), glucosamine (GlcN), glucose (Glc), galactose (Gal) and mannose (Man) at a 500 µM concentration in HBS buffer (10 mM HEPES, 140 mM NaCl, pH 7.4) was monitored on Biacore T100.

177x122mm (300 x 300 DPI)

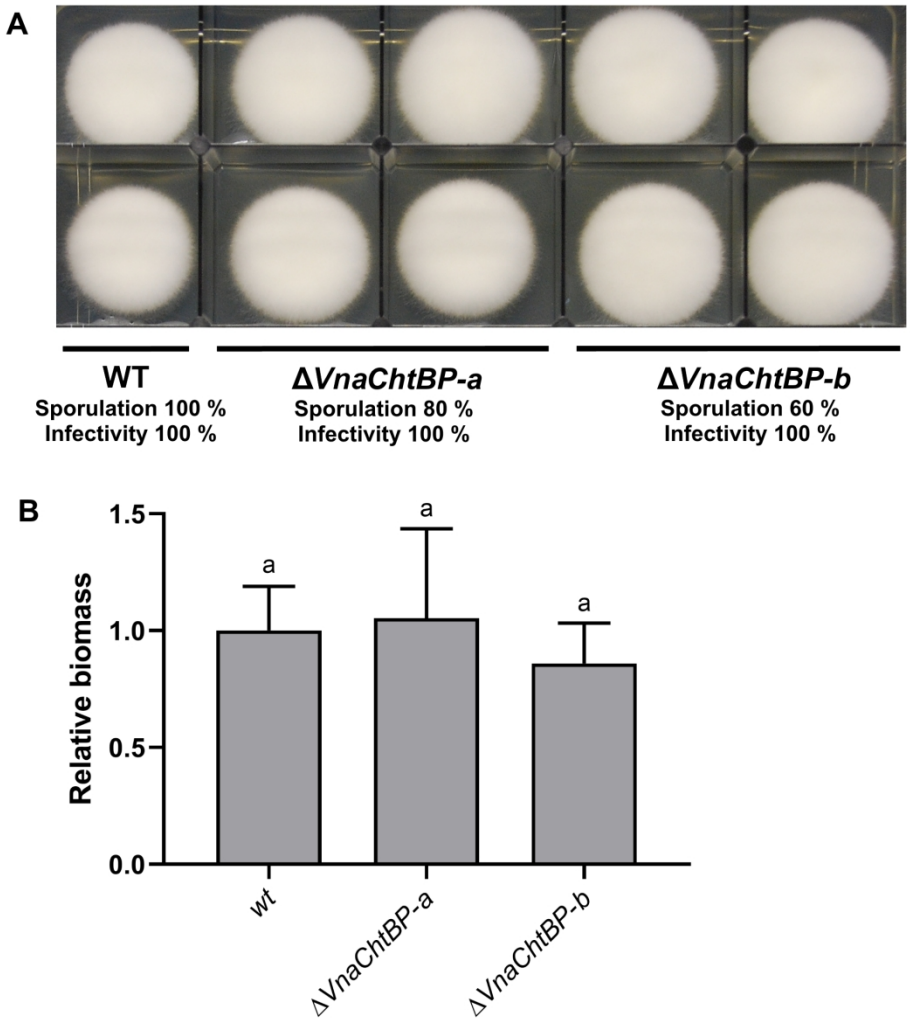

The morphology, sporulation and infectivity of *Verticillium nonalfalfae* wild type and *VnaChtBP* knockout mutants (A) and relative fungal biomass quantification in infected hop (B). Sporulation assessment 5 denotes 100% conidiation, while 1 denotes 20% conidiation of the wild type. Infectivity of 100% means all plants were infected with *V. nonalfalfae* as determined by fungal re-isolation from infected hop. The relative quantity of *V. nonalfalfae* DNA in infected hop was estimated at 21 dpi with the $2^{-\Delta\Delta C}{}_{t}$ method (Schmittgen and Livak 2008) using *V. nonalfalfae* lethal genotype (PG2) specific primer 5-1gs (Radišek et al. 2004) and hop reference gene *DRH1* (DEAD box RNA helicase) for normalization (Štajner et al. 2013). Amplification levels are expressed relative to those obtained from plants infected with the wild type strain. One-way ANOVA with Tukey's multiple comparison test was performed in GraphPad Prism 8.02 (GraphPad Software, San Diego, California USA, www.graphpad.com) to test for difference between the wild type and mutant group means.

177x193mm (300 x 300 DPI)